

---

# SegDAC: Segmentation-Driven Actor-Critic for Visual Reinforcement Learning

**Alexandre Brown**  
alexandre.brown@mila.quebec  
Mila Quebec AI Institute  
Université de Montréal

**Glen Berseth**  
glen.berseth@mila.quebec  
Mila Quebec AI Institute  
Université de Montréal

## Abstract

Visual reinforcement learning (RL) is challenging due to the need to learn both perception and actions from high-dimensional inputs and noisy rewards. Although large perception models exist, integrating them effectively into RL for visual generalization and improved sample efficiency remains unclear. We propose **SegDAC**, a **Segmentation-Driven Actor-Critic** method. SegDAC uses Segment Anything (SAM) for object-centric decomposition and YOLO-World to ground segments semantically via text prompts. It includes a novel transformer-based architecture that supports a dynamic number of segments at each time step and effectively learns which segments to focus on using online RL, without using human labels. By evaluating SegDAC over a challenging visual generalization benchmark using Maniskill3, which covers diverse manipulation tasks under strong visual perturbations, we demonstrate that SegDAC achieves significantly better visual generalization, doubling prior performance on the hardest setting and matching or surpassing prior methods in sample efficiency across all evaluated tasks. **Project Page:** <https://segdac.github.io/>

## 1 Introduction

Reinforcement learning (RL) from images is challenging because of the high dimensionality of visual inputs, their diversity and the limited generalization to visual perturbations (Mnih et al., 2013; Pathak et al., 2017; Yarats et al., 2020; Lepert et al., 2024; Yuan et al., 2023; Lyu et al., 2024; Lepert et al., 2024). A possible solution to overcoming the challenge of high dimensionality is to leverage pre-trained visual models, however, it has been difficult to adapt these models due to their complexity in both identifying the optimal model layer to feed into the policy and mitigating the inference cost for larger models applied to RL problems that require extensive experience collection.

To overcome the above issues, we introduce **SegDAC** (**Segmentation-Driven Actor-Critic**), a novel RL method that incorporates segmentation into the actor-critic framework (Mnih et al., 2013; Konda and Tsitsiklis, 1999). Instead of learning from raw pixels or patches, SegDAC uses semantic masks to process input at the level of image segments. This aligns better with human perception and provides a more abstract, structured representation that improves both generalization and sample efficiency (Chen et al., 2024; Locatello et al., 2020; Wang et al., 2023).

Our method introduces a transformer-based actor-critic architecture that handles a variable number of segment embeddings per frame, learning entirely in latent space. We use text prompts to semantically ground Segment Anything (SAM) predictions, shifting RL from pixel-level to semantic-level reasoning. SegDAC can augment standard model-free RL algorithms like DDPG Lillicrap et al. (2019), TD3 Fujimoto et al. (2018), and SAC Haarnoja

---

et al. (2018; 2019), without requiring human-labelled segmentation or assumptions on segment count or resolution. SegDAC, unlike previous ViT-based visual RL approaches Tao et al. (2022), exceeds CNN-based methods in sample efficiency and significantly outperforms them in visual generalization, directly challenging the belief that ViTs are less effective in online RL.

To further evaluate SegDAC in comparison to prior work, we construct a challenging visual generalization benchmark built on ManiSkill3 Tao et al. (2024), with strong out-of-distribution visual perturbations across diverse manipulation tasks. This addresses the limitations of simpler benchmarks like Deep Mind Control Generalization Benchmark (DMC-GB) Hansen et al. (2021), which often fail to reflect more realistic visual complexity Yuan et al. (2023). Overall, SegDAC establishes a new state-of-the-art in visual generalization, outperforming prior methods by up to  $2\times$  under the most challenging perturbation settings, while matching or exceeding their sample efficiency across all evaluated tasks.

## 2 Related Work

**RL from Images.** Learning policies directly from pixels is sample-inefficient and suffers from generalization issues due to the high-dimensional nature of images (Mnih et al., 2013; Yarats et al., 2020; Lyu et al., 2024). SAC-AE (Yarats et al., 2020) and auxiliary losses (Jaderberg et al., 2016) partially address this. In contrast, SegDAC does not use auxiliary losses and processes images at the segment level, resulting in more abstract and robust representations.

**Pretrained Models and Data Augmentation in RL.** Pretrained representations have been used to boost RL performance (Wang et al., 2023; Yuan et al., 2022; Russakovsky et al., 2015; Ricciardi et al., 2024; Hansen et al., 2021). Some works rely on world models (Garrido et al., 2024; Hafner et al., 2022), multi-view losses (Yuan et al., 2024; Haramati et al., 2024), or data augmentations (Almuzairee et al., 2024; Hansen et al., 2021; Hansen and Wang, 2021; Bertoin et al., 2023; Yuan et al., 2022; Kostrikov et al., 2021; Yarats et al., 2021; Laskin et al., 2020). SegDAC differs significantly by avoiding data augmentation and auxiliary datasets/tasks, instead directly integrating a segmentation-driven architecture that leverages SAM encoder’s latent representation in a novel object-centric way. Many approaches rely on expert data or multi-phase training (Hoang et al., 2023; Liu et al., 2025; Goyal et al., 2023; 2024; Fang et al., 2025). SegDAC is trained purely using online RL in a model-free setting, without labels/demonstrations or offline datasets.

**Segmentation for RL.** Melnik et al. (2021) uses RL to train a segmentation model, while SegDAC inverts this paradigm by using segmentation to guide the RL process. Saliency-based approaches (Wu et al., 2021; Bertoin et al., 2023; Wu et al., 2021; Wang et al., 2021; Liang et al., 2024; Grooten et al., 2023) focus on pixel-level importance, lacking semantic abstraction. Other works depend on human annotations or assume a fixed number of segments per frame (Wang et al., 2023; Liang et al., 2024; Chen et al., 2024). Chen et al. (2024) selects a fixed number of segments using a simple mean attention score over a static grid of points to get segments from SAM and reconstructs a full RGB image, continuing to learn in pixel space with a CNN. In contrast, SegDAC uses YOLO-World to semantically guide SAM via text prompts, and introduces a novel module that extracts a variable-length sequence of segment embeddings directly from SAM’s encoder Zhang et al. (2024). SegDAC operates entirely in latent space using pretrained embeddings, and applies true multi-head attention Vaswani et al. (2023) for richer inter-segment reasoning.

## 3 Background

Visual reinforcement learning (RL) is commonly formulated as a Partially Observable Markov Decision Process (POMDP) Littman (2009), where the agent receives high-

dimensional image observations without access to the full environment state. A POMDP is defined by  $(S, O, A, T, R, \gamma)$ , where  $S$  is the state space,  $O$  the observation space (e.g., RGB images),  $A$  the action space,  $T$  the unknown transition function,  $R$  the reward function,  $\gamma \in [0, 1]$  the discount factor, and  $H$  the time horizon. The objective is to learn a policy  $\pi : O \mapsto A$  that maximizes the expected return:  $\mathbb{E}_\pi \left[ \sum_{t=0}^H \gamma^t r_t \right]$ . In this work, we focus on online, model-free visual RL using Soft Actor-Critic (SAC) Haarnoja et al. (2018; 2019) as our base algorithm, a widely used actor-critic algorithm for visual RL in continuous control (Yarats et al., 2020; Laskin et al., 2020; Kostrikov et al., 2021; Hansen and Wang, 2021; Hansen et al., 2021; Bertoin et al., 2023; Yuan et al., 2022; Grooten et al., 2023; Chen et al., 2024; Almuzairee et al., 2024). SAC jointly maximizes the expected return and policy entropy. The critic minimizes the Bellman residual, and the actor maximizes the critic’s Q-value under the current policy. Unlike standard visual RL pipelines that use stacked image frames, we extract segment embeddings from 1 frame at each time step and process them as a variable-length sequence.

## 4 Method

An overview of SegDAC is shown in Figure 1. Given an RGB image and a set of grounding text tags, the grounded segmentation module (section 4.1) uses YOLO-World Cheng et al. (2024) to generate bounding boxes based on the text prompts and EfficientViT-SAM Zhang et al. (2024) to produce segment masks and patch embeddings. The segment embedding extraction module (section 4.2) extracts features within each mask to form a variable-length sequence of segment embeddings, which is then passed to a transformer-based actor (section 4.3) or critic (section 4.4) to predict actions or Q-values.

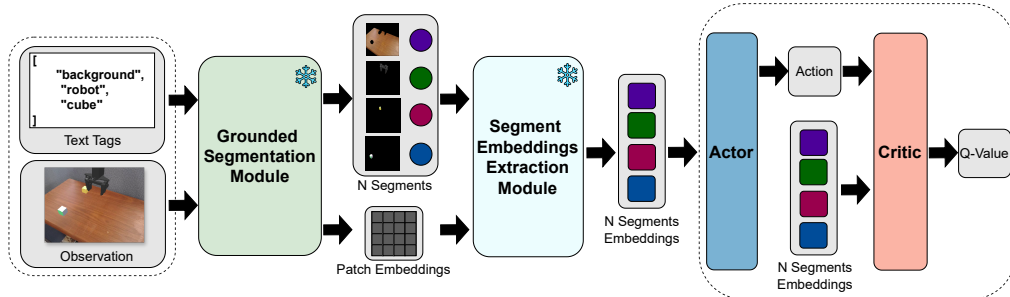


Figure 1: SegDAC overview.

Operating directly on segment embeddings enables reasoning over semantically meaningful regions while avoiding pixel-level noise. Further details on the grounded segmentation module and segment embeddings extraction module are provided in the next section. See the appendix for text prompt definitions and implementation specifics.

### 4.1 Grounded Segmentation Module

Our grounded segmentation module, shown in Figure 2, is inspired by Grounded SAM Ren et al. (2024), which combines Grounding DINO Liu et al. (2024) with SAM Kirillov et al. (2023) for text-guided segmentation. However, we found it too slow for online RL. Instead, we adopt a faster pipeline: YOLO-World Cheng et al. (2024) generates bounding boxes from text prompts and EfficientViT-SAM Zhang et al. (2024) extracts segments within those boxes. For simplicity, we refer to EfficientViT-SAM as SAM throughout the rest of the paper. A key characteristic of our module is that the number of output segments,  $N$ , is variable across different time steps, unlike methods that operate on a fixed number of object representations (Chen et al., 2024; Locatello et al., 2020; Shi et al., 2024; Daniel and Tamar, 2022).

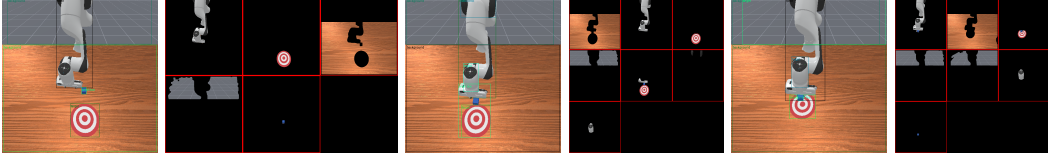


Figure 3: Examples of grounded segments for the PushCube task. Left: image with YOLO-World bounding boxes. Right: segments extracted by EfficientViT-SAM using boxes.

To avoid the inefficiency and potential randomness of prompt-free "segment anything" approaches, which rely on a dense static grid of points and often require heavy post-processing, we instead use prompt-based segmentation. YOLO-World, an open-vocabulary object detector, predicts  $K$  bounding boxes from an image given a set of text prompts. These boxes are passed to SAM, which produces  $N$  segments per frame, where  $N$  varies depending on the input. This approach encourages SAM to focus on task-relevant objects, resulting in more semantically grounded segmentations. For efficiency, we reuse the SAM encoder’s patch embeddings, leveraging its strong pretrained representations (Zhang et al., 2024; Kirillov et al., 2023). Both YOLO-World and SAM remain frozen during RL training and inference.

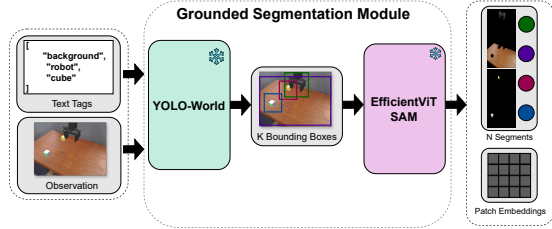


Figure 2: Our grounded segmentation module leverages the strengths of both YOLO-World and EfficientViT-SAM models to efficiently detect segments from the image.

Figure 3 shows examples of the grounded segments extracted for the PushCube-v1 task. While YOLO-World’s predictions are not always perfect, they effectively decompose the scene into bounding boxes based on the text tags. Notably, incorrect label predictions do not affect segmentation quality, as SAM relies only on bounding box coordinates, helping avoid compounding errors.

Motivated by our ablation experiments in the appendix (B.1), we include “background” in the text prompts to encourage detection of additional segments. This incentivizes the agent to ignore irrelevant segments, thereby improving generalization compared to using only task-specific prompts. Due to computational constraints, we selected broad prompts that performed reasonably well with SAM on a static image.

## 4.2 Segment Embeddings Extraction Module

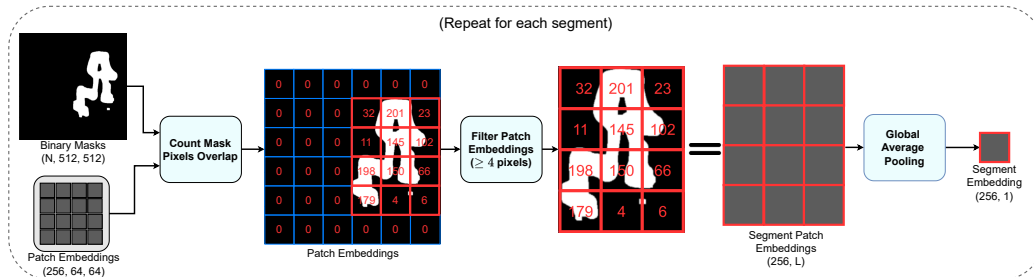


Figure 4: Segment embedding extraction: For each SAM-predicted mask, we select patch embeddings with sufficient overlap ( $\geq 4$  pixels), then apply global average pooling to obtain one embedding per segment.

The segment embedding extraction module takes as input  $N$  binary segmentation masks and the patch embeddings from the SAM encoder and outputs  $N$  segment embeddings where  $N$  varies per frame. This module in Figure 4 has no trainable parameters.

To compute a segment embedding, we identify the patch embeddings that spatially overlap with the segment’s binary mask. For each patch, we count the number of active (value=1) pixels from the mask within the patch boundary. Patches with fewer than a threshold (e.g., 4 pixels) are discarded. We then apply global average pooling over the remaining relevant patch embeddings to produce a single embedding vector of dimension  $S$  (e.g:  $S = 256$ ). This process is repeated independently for each of the  $N$  masks.

An analysis of the segment embedding extraction process including patch overlap heatmap, mask-patch alignment is provided in the appendix (F).

### 4.3 Actor Network

The actor network (Figure 5) maps segment embeddings and proprioceptive inputs to action distribution parameters. It receives a variable number ( $N$ ) of segment embeddings of dimension  $S$  and the proprioception data of dimension  $P$ , using only joint positions for real-world applicability. Both inputs are linearly projected to a common dimension  $D$ , and token type encodings (for the query, segment, and proprioception) are added.

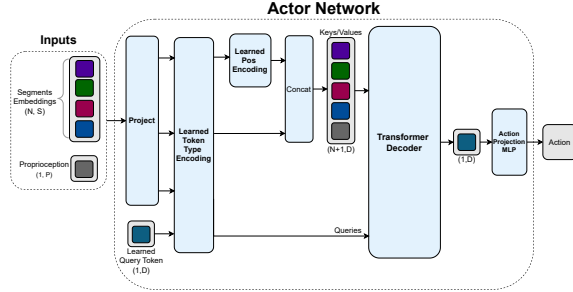


Figure 5: SegDAC actor network architecture.

To encode spatial information, we follow [Chen et al. \(2025\)](#) and compute positional encodings from segment bounding box coordinates via a small learned MLP, which are added to the segment embeddings. The combined segment and proprioceptive tokens form the keys and values for our transformer decoder [Vaswani et al. \(2023\)](#), while a learned query token serves as the query input.

The decoder uses multi-head self- and cross-attention to contextualize the query, which is then passed through an MLP that outputs a tensor of size  $2 \times A$ , corresponding to the mean and standard deviation of the action distribution in SAC. The architecture is modular and can be adapted to other algorithms (e.g: TD3) by adjusting the output layer dimension.

### 4.4 Critic Network

The critic network (Figure 6) estimates the Q-value given segment embeddings, proprioceptive information and an action. All of these inputs are each projected to a shared dimension  $D$ . Token type encodings are added to all inputs, and segment embeddings receive additional positional encodings via a learned MLP from bounding box coordinates, as in the actor. Segment and proprioception tokens form the keys ( $K$ ) and values ( $V$ ) for the transformer decoder. In contrast to the actor, the action is concatenated with a learned token and passed through an MLP to produce a query token. The transformer decoder contextualizes this query, and a final MLP projects the output to a scalar Q-value, compatible with model-free RL algorithms such as SAC or TD3.

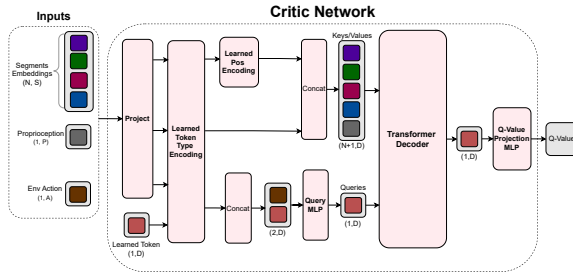


Figure 6: SegDAC critic network architecture.

---

## 5 Experiments

To evaluate the benefits of SegDAC, we conduct extensive experiments. We first introduce a new visual generalization benchmark based on ManiSkill3 [Tao et al. \(2024\)](#), which defines three difficulty levels: easy, medium, and hard, using clear criteria rather than random parameter sampling. We compare SegDAC to state-of-the-art baselines on this benchmark and provide an attention analysis showing how it attends to different image segments when predicting Q-values. We also analyze sample efficiency and refer to the appendix (G) for a detailed study of SegDAC’s robustness to segment variability.

**Training, Evaluation and Testing Methodology** Inspired by prior model-free online visual RL work ([Hansen et al., 2021](#); [Almuzairee et al., 2024](#)), all methods were trained for 1M environment steps without visual perturbations across 8 robotic manipulation tasks. These tasks cover a diverse range of visual appearances, object configurations, and difficulty levels and involve both the Franka Emika Panda arm and the Unitree G1 humanoid robot. Policy evaluation is performed every 10K steps on a separate, unperturbed environment with a different seed, averaging metrics over 10 rollouts and 5 seeds. Hyperparameters were the same for all tasks, except for task-specific text prompts. To test visual generalization, we introduce a benchmark extending ManiSkill3 for 8 tasks, 3 difficulty levels, and 12 visual perturbations. Each visual perturbation test for each task and each difficulty was tested with 5 seeds and 50 rollouts, reporting IQM returns and 95% confidence intervals following [Agarwal et al. \(2022\)](#). Additional details in the appendix.

### 5.1 Visual Generalization Benchmark and Results

Inspired by The Colosseum benchmark [Pumacay et al. \(2024\)](#), we define the following taxonomy of scene entities:

1. **Manipulation Object (MO):** The task-critical object directly grasped or moved by the robot’s end-effector to complete the main objective.
2. **Receiver Object (RO):** An essential object not directly manipulated, but necessary for task completion by interacting with the MO.
3. **Primary Interaction Surface (Table):** The main horizontal surface that supports or anchors interactions between MOs and ROs.
4. **Background Elements:** All other visual components not classified above (e.g., walls, peripheral floor, skybox, distant scenery).

**Visual perturbation categories** include:

(1) camera (pose, field of view), (2) lighting (direction, color), (3) color (MO, RO, table, background) and (4) texture (MO, RO, table, background).

**Difficulty levels:** Each individual perturbation is evaluated at three difficulty levels:

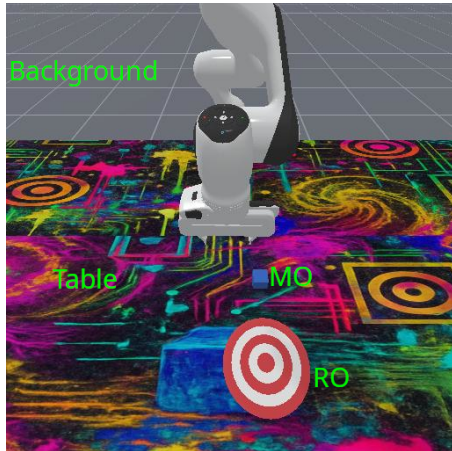


Figure 7: Example of a hard visual perturbation in the PushCube task. The table texture contains challenging patterns resembling cubes and targets, which can visually and semantically conflict with the real manipulation object (MO) and receiver object (RO). Scene entities are labeled following our defined taxonomy for illustration purposes.

**Easy** introduces minor visual changes that remain close to the default configuration and maintain strong visual similarity. These serve as smoke tests to verify robustness to small, non-disruptive variations.

**Medium** introduces substantial visual changes with low similarity to the default view, while remaining neutral and task-valid. Perturbations are designed to avoid semantic conflicts between scene entities (e.g., avoiding textures or colors that could alter an entity’s semantic meaning). These configurations are visually distinct, yet realistic and solvable.

**Hard** applies aggressive, out-of-distribution perturbations that introduce visually and semantically challenging cues. These configurations differ significantly from the default view, with extreme changes in camera angles, lighting, colors, or textures that may confuse the agent’s perception (e.g., a cube with the same texture as the target). They are intentionally sub-optimal and would not be selected when aiming to facilitate task completion.

We refer the reader to the appendix (A) for extensive details on the benchmark definition, quantitative and qualitative results of the tasks and perturbations for the various difficulties.

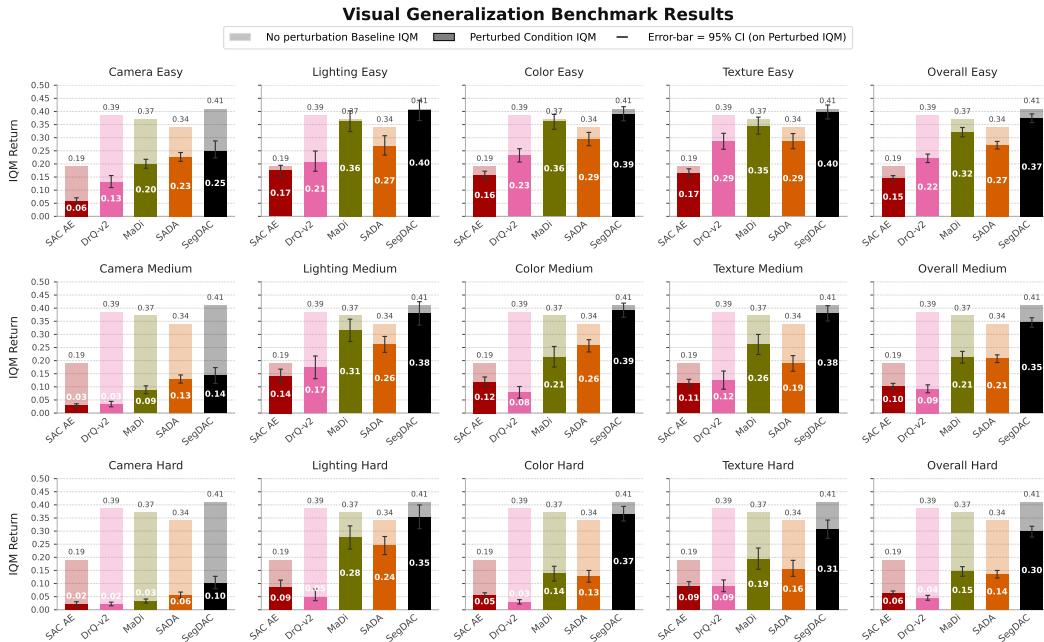


Figure 8: Visual generalization results grouped by categories.

**Results:** We evaluate four visual RL baselines: SAC-AE [Yarats et al. \(2020\)](#) as a lower bound, DrQ-v2 [Yarats et al. \(2021\)](#) as a state-of-the-art in sample efficiency, MaDi [Grooten et al. \(2023\)](#) and SADA [Almuzaire et al. \(2024\)](#) as strong methods in visual generalization.

As shown by Figure 8, SegDAC consistently outperforms all baselines across difficulty levels and perturbation categories. While most baselines maintain reasonable performance under easy perturbations, their performance degrades sharply in medium and hard settings. In contrast, SegDAC retains strong performance even under severe distribution shifts. For example, in the hardest setting, MaDi drops from 0.37 to 0.15 IQM (−0.22), while SegDAC only drops from 0.41 to 0.30 (−0.11), achieving approximately twice the performance of both MaDi and SADA. This widening gap highlights the superior robustness of our approach as visual perturbations become more challenging. Although DrQ-v2 remains competitive in terms of sample efficiency (see Figure 10), it shows poor generalization under visual perturbations, with a sharp drop in IQM return even at the easy difficulty level. Notably, all methods struggle in the camera hard setting, suggesting limitations in current single-view architectures. Addressing viewpoint sensitivity through multi-view or viewpoint-invariant approaches is a promising direction for future work.

## 5.2 Segment Attention Analysis

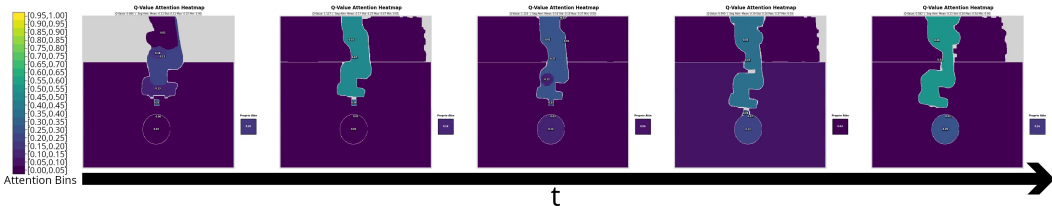


Figure 9: Critic attention on visual segments and proprioception during Q-value prediction (Push Cube task).

Figure 9 and extensive qualitative examples in the appendix (H) demonstrates that SegDAC selectively attends to task-relevant objects while ignoring irrelevant segments, such as background or the table. Without history or frame stacking, it adapts attention over time focusing on the robot arm and cube at the start, then starts paying attention to the target after grasping the cube. The policy remains robust to changes in segment count and temporary loss of key segments as shown in the appendix (G).

## 5.3 Sample Efficiency

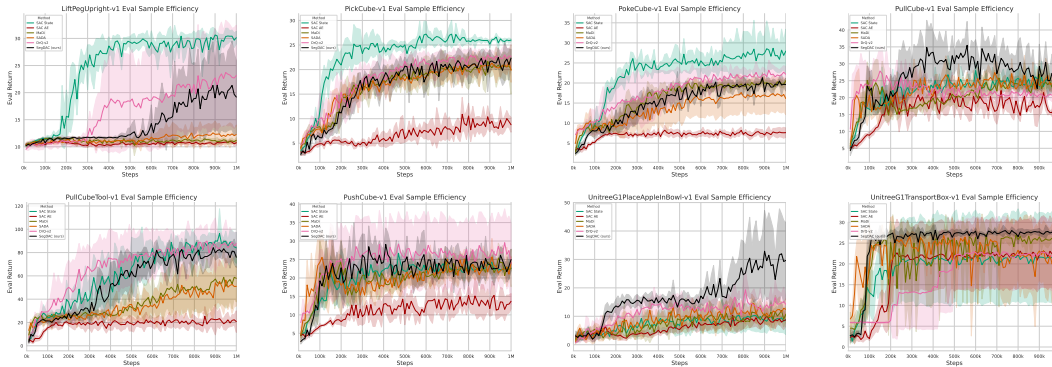


Figure 10: Evaluation return sample efficiency curves for all 8 manipulation tasks.

To assess the sample efficiency of SegDAC, we compare it to the same baselines used in the visual generalization benchmark, with the addition of an MLP-based SAC model Haarnoja et al. (2018; 2019) trained on privileged state information to approximate oracle performance as an upper bound. Figure 10 demonstrates that SegDAC matches the sample efficiency of the previous state-of-the-art DrQ-v2 across all tasks and outperforms it in three out of eight tasks. Importantly, SegDAC consistently achieves higher sample efficiency than the visual generalization baselines (MaDi, SADA) on every task.

## 6 Discussion

We introduced SegDAC, a novel actor-critic architecture that efficiently integrates pre-trained perception with text-grounded, object-centric segmentation to model relationships among variable image segments. The results are evaluated across multiple manipulation tasks with different robots. SegDAC achieves strong performance without relying on frame stacking, data augmentation, human labels, or auxiliary tasks. While this work focuses on short-horizon online RL, extending SegDAC to longer horizons, alternative learning paradigms and real-world deployment is a promising direction. However, SegDAC improves both visual generalization and sample efficiency and remains robust even when image regions are missing.

---

## References

- V. Mnih, K. Kavukcuoglu, D. Silver, A. Graves, I. Antonoglou, D. Wierstra, and M. Riedmiller. Playing atari with deep reinforcement learning, 2013. URL <https://arxiv.org/abs/1312.5602>.
- D. Pathak, P. Agrawal, A. A. Efros, and T. Darrell. Curiosity-driven exploration by self-supervised prediction, 2017. URL <https://arxiv.org/abs/1705.05363>.
- D. Yarats, A. Zhang, I. Kostrikov, B. Amos, J. Pineau, and R. Fergus. Improving sample efficiency in model-free reinforcement learning from images, 2020. URL <https://arxiv.org/abs/1910.01741>.
- M. Lepert, R. Doshi, and J. Bohg. Shadow: Leveraging segmentation masks for zero-shot cross-embodiment policy transfer. In Conference on Robot Learning (CoRL), Munich, Germany, 2024.
- Z. Yuan, S. Yang, P. Hua, C. Chang, K. Hu, and H. Xu. Rl-vigen: A reinforcement learning benchmark for visual generalization, 2023. URL <https://arxiv.org/abs/2307.10224>.
- J. Lyu, L. Wan, X. Li, and Z. Lu. Understanding what affects generalization gap in visual reinforcement learning: Theory and empirical evidence, 2024. URL <https://arxiv.org/abs/2402.02701>.
- V. Konda and J. Tsitsiklis. Actor-critic algorithms. In S. Solla, T. Leen, and K. Müller, editors, Advances in Neural Information Processing Systems, volume 12. MIT Press, 1999. URL [https://proceedings.neurips.cc/paper\\_files/paper/1999/file/6449f44a102fde848669bdd9eb6b76fa-Paper.pdf](https://proceedings.neurips.cc/paper_files/paper/1999/file/6449f44a102fde848669bdd9eb6b76fa-Paper.pdf).
- C. Chen, J. Xu, W. Liao, H. Ding, Z. Zhang, Y. Yu, and R. Zhao. Focus-then-decide: Segmentation-assisted reinforcement learning. Proceedings of the AAAI Conference on Artificial Intelligence, 38(10):11240–11248, Mar. 2024. doi:10.1609/aaai.v38i10.29002. URL <https://ojs.aaai.org/index.php/AAAI/article/view/29002>.
- F. Locatello, D. Weissenborn, T. Unterthiner, A. Mahendran, G. Heigold, J. Uszkoreit, A. Dosovitskiy, and T. Kipf. Object-centric learning with slot attention, 2020. URL <https://arxiv.org/abs/2006.15055>.
- Z. Wang, Y. Ze, Y. Sun, Z. Yuan, and H. Xu. Generalizable visual reinforcement learning with segment anything model, 2023. URL <https://arxiv.org/abs/2312.17116>.
- T. P. Lillicrap, J. J. Hunt, A. Pritzel, N. Heess, T. Erez, Y. Tassa, D. Silver, and D. Wierstra. Continuous control with deep reinforcement learning, 2019. URL <https://arxiv.org/abs/1509.02971>.
- S. Fujimoto, H. van Hoof, and D. Meger. Addressing function approximation error in actor-critic methods, 2018. URL <https://arxiv.org/abs/1802.09477>.
- T. Haarnoja, A. Zhou, P. Abbeel, and S. Levine. Soft actor-critic: Off-policy maximum entropy deep reinforcement learning with a stochastic actor, 2018. URL <https://arxiv.org/abs/1801.01290>.
- T. Haarnoja, A. Zhou, K. Hartikainen, G. Tucker, S. Ha, J. Tan, V. Kumar, H. Zhu, A. Gupta, P. Abbeel, and S. Levine. Soft actor-critic algorithms and applications, 2019. URL <https://arxiv.org/abs/1812.05905>.
- T. Tao, D. Reda, and M. van de Panne. Evaluating vision transformer methods for deep reinforcement learning from pixels, 2022. URL <https://arxiv.org/abs/2204.04905>.

- 
- S. Tao, F. Xiang, A. Shukla, Y. Qin, X. Hinrichsen, X. Yuan, C. Bao, X. Lin, Y. Liu, T. kai Chan, Y. Gao, X. Li, T. Mu, N. Xiao, A. Gurha, Z. Huang, R. Calandra, R. Chen, S. Luo, and H. Su. Maniskill3: Gpu parallelized robotics simulation and rendering for generalizable embodied ai, 2024. URL <https://arxiv.org/abs/2410.00425>.
- N. Hansen, H. Su, and X. Wang. Stabilizing deep q-learning with convnets and vision transformers under data augmentation, 2021. URL <https://arxiv.org/abs/2107.00644>.
- M. Jaderberg, V. Mnih, W. M. Czarnecki, T. Schaul, J. Z. Leibo, D. Silver, and K. Kavukcuoglu. Reinforcement learning with unsupervised auxiliary tasks, 2016. URL <https://arxiv.org/abs/1611.05397>.
- Z. Yuan, Z. Xue, B. Yuan, X. Wang, Y. Wu, Y. Gao, and H. Xu. Pre-trained image encoder for generalizable visual reinforcement learning, 2022. URL <https://arxiv.org/abs/2212.08860>.
- O. Russakovsky, J. Deng, H. Su, J. Krause, S. Satheesh, S. Ma, Z. Huang, A. Karpathy, A. Khosla, M. Bernstein, A. C. Berg, and L. Fei-Fei. Imagenet large scale visual recognition challenge, 2015. URL <https://arxiv.org/abs/1409.0575>.
- A. P. Ricciardi, V. Maiorca, L. Moschella, R. Marin, and E. Rodolà. Zero-shot stitching in reinforcement learning using relative representations, 2024. URL <https://arxiv.org/abs/2404.12917>.
- N. Hansen, R. Jangir, Y. Sun, G. Alenyà, P. Abbeel, A. A. Efros, L. Pinto, and X. Wang. Self-supervised policy adaptation during deployment, 2021. URL <https://arxiv.org/abs/2007.04309>.
- Q. Garrido, M. Assran, N. Ballas, A. Bardes, L. Najman, and Y. LeCun. Learning and leveraging world models in visual representation learning, 2024. URL <https://arxiv.org/abs/2403.00504>.
- D. Hafner, K.-H. Lee, I. Fischer, and P. Abbeel. Deep hierarchical planning from pixels, 2022. URL <https://arxiv.org/abs/2206.04114>.
- Z. Yuan, T. Wei, S. Cheng, G. Zhang, Y. Chen, and H. Xu. Learning to manipulate anywhere: A visual generalizable framework for reinforcement learning, 2024. URL <https://arxiv.org/abs/2407.15815>.
- D. Haramati, T. Daniel, and A. Tamar. Entity-centric reinforcement learning for object manipulation from pixels, 2024. URL <https://arxiv.org/abs/2404.01220>.
- A. Almuzairee, N. Hansen, and H. I. Christensen. A recipe for unbounded data augmentation in visual reinforcement learning, 2024. URL <https://arxiv.org/abs/2405.17416>.
- N. Hansen and X. Wang. Generalization in reinforcement learning by soft data augmentation, 2021. URL <https://arxiv.org/abs/2011.13389>.
- D. Bertoin, A. Zouitine, M. Zouitine, and E. Rachelson. Look where you look! saliency-guided q-networks for generalization in visual reinforcement learning, 2023. URL <https://arxiv.org/abs/2209.09203>.
- I. Kostrikov, D. Yarats, and R. Fergus. Image augmentation is all you need: Regularizing deep reinforcement learning from pixels, 2021. URL <https://arxiv.org/abs/2004.13649>.
- D. Yarats, R. Fergus, A. Lazaric, and L. Pinto. Mastering visual continuous control: Improved data-augmented reinforcement learning, 2021. URL <https://arxiv.org/abs/2107.09645>.

- 
- M. Laskin, K. Lee, A. Stooke, L. Pinto, P. Abbeel, and A. Srinivas. Reinforcement learning with augmented data, 2020. URL <https://arxiv.org/abs/2004.14990>.
- M.-H. Hoang, L. Dinh, and H. Nguyen. Learning from pixels with expert observations, 2023. URL <https://arxiv.org/abs/2306.13872>.
- J. Liu, H. Chen, P. An, Z. Liu, R. Zhang, C. Gu, X. Li, Z. Guo, S. Chen, M. Liu, C. Hou, M. Zhao, K. alex Zhou, P.-A. Heng, and S. Zhang. Hybridvla: Collaborative diffusion and autoregression in a unified vision-language-action model, 2025. URL <https://arxiv.org/abs/2503.10631>.
- A. Goyal, J. Xu, Y. Guo, V. Blukis, Y.-W. Chao, and D. Fox. Rvt: Robotic view transformer for 3d object manipulation, 2023. URL <https://arxiv.org/abs/2306.14896>.
- A. Goyal, V. Blukis, J. Xu, Y. Guo, Y.-W. Chao, and D. Fox. Rvt-2: Learning precise manipulation from few demonstrations, 2024. URL <https://arxiv.org/abs/2406.08545>.
- H. Fang, M. Grotz, W. Pumacay, Y. R. Wang, D. Fox, R. Krishna, and J. Duan. Sam2act: Integrating visual foundation model with a memory architecture for robotic manipulation, 2025. URL <https://arxiv.org/abs/2501.18564>.
- A. Melnik, A. Harter, C. Limberg, K. Rana, N. Suenderhauf, and H. Ritter. Critic guided segmentation of rewarding objects in first-person views, 2021. URL <https://arxiv.org/abs/2107.09540>.
- H. Wu, K. Khetarpal, and D. Precup. Self-supervised attention-aware reinforcement learning. *Proceedings of the AAAI Conference on Artificial Intelligence*, 35(12):10311–10319, May 2021. doi:10.1609/aaai.v35i12.17235. URL <https://ojs.aaai.org/index.php/AAAI/article/view/17235>.
- X. Wang, L. Lian, and S. X. Yu. Unsupervised visual attention and invariance for reinforcement learning, 2021. URL <https://arxiv.org/abs/2104.02921>.
- A. Liang, J. Thomason, and E. Byrk. Visarl: Visual reinforcement learning guided by human saliency, 2024. URL <https://arxiv.org/abs/2403.10940>.
- B. Grooten, T. Tomilin, G. Vasan, M. E. Taylor, A. R. Mahmood, M. Fang, M. Pechenizkiy, and D. C. Mocanu. Madi: Learning to mask distractions for generalization in visual deep reinforcement learning, 2023. URL <https://arxiv.org/abs/2312.15339>.
- Z. Zhang, H. Cai, and S. Han. Efficientvit-sam: Accelerated segment anything model without accuracy loss, 2024. URL <https://arxiv.org/abs/2402.05008>.
- A. Vaswani, N. Shazeer, N. Parmar, J. Uszkoreit, L. Jones, A. N. Gomez, L. Kaiser, and I. Polosukhin. Attention is all you need, 2023. URL <https://arxiv.org/abs/1706.03762>.
- M. L. Littman. A tutorial on partially observable markov decision processes. *Journal of Mathematical Psychology*, 53(3):119–125, 2009. ISSN 0022-2496. doi:<https://doi.org/10.1016/j.jmp.2009.01.005>. URL <https://www.sciencedirect.com/science/article/pii/S0022249609000042>. Special Issue: Dynamic Decision Making.
- T. Cheng, L. Song, Y. Ge, W. Liu, X. Wang, and Y. Shan. Yolo-world: Real-time open-vocabulary object detection, 2024. URL <https://arxiv.org/abs/2401.17270>.
- T. Ren, S. Liu, A. Zeng, J. Lin, K. Li, H. Cao, J. Chen, X. Huang, Y. Chen, F. Yan, Z. Zeng, H. Zhang, F. Li, J. Yang, H. Li, Q. Jiang, and L. Zhang. Grounded sam: Assembling open-world models for diverse visual tasks, 2024. URL <https://arxiv.org/abs/2401.14159>.

- 
- S. Liu, Z. Zeng, T. Ren, F. Li, H. Zhang, J. Yang, Q. Jiang, C. Li, J. Yang, H. Su, J. Zhu, and L. Zhang. Grounding dino: Marrying dino with grounded pre-training for open-set object detection, 2024. URL <https://arxiv.org/abs/2303.05499>.
- A. Kirillov, E. Mintun, N. Ravi, H. Mao, C. Rolland, L. Gustafson, T. Xiao, S. Whitehead, A. C. Berg, W.-Y. Lo, P. Dollár, and R. Girshick. Segment anything, 2023. URL <https://arxiv.org/abs/2304.02643>.
- J. Shi, J. Qian, Y. J. Ma, and D. Jayaraman. Composing pre-trained object-centric representations for robotics from "what" and "where" foundation models, 2024. URL <https://arxiv.org/abs/2404.13474>.
- T. Daniel and A. Tamar. Unsupervised image representation learning with deep latent particles, 2022. URL <https://arxiv.org/abs/2205.15821>.
- D. Chen, S. Cahyawijaya, J. Liu, B. Wang, and P. Fung. Subobject-level image tokenization, 2025. URL <https://arxiv.org/abs/2402.14327>.
- R. Agarwal, M. Schwarzer, P. S. Castro, A. Courville, and M. G. Bellemare. Deep reinforcement learning at the edge of the statistical precipice, 2022. URL <https://arxiv.org/abs/2108.13264>.
- W. Pumacay, I. Singh, J. Duan, R. Krishna, J. Thomason, and D. Fox. The colosseum: A benchmark for evaluating generalization for robotic manipulation, 2024. URL <https://arxiv.org/abs/2402.08191>.
- Y. Zhang, X. Huang, J. Ma, Z. Li, Z. Luo, Y. Xie, Y. Qin, T. Luo, Y. Li, S. Liu, Y. Guo, and L. Zhang. Recognize anything: A strong image tagging model, 2023a. URL <https://arxiv.org/abs/2306.03514>.
- R. Zhang, Z. Jiang, Z. Guo, S. Yan, J. Pan, X. Ma, H. Dong, P. Gao, and H. Li. Personalize segment anything model with one shot, 2023b. URL <https://arxiv.org/abs/2305.03048>.
- K. Sreedhar. Enhancement of images using morphological transformations. *International Journal of Computer Science and Information Technology*, 4(1):33–50, Feb. 2012. ISSN 0975-4660. doi:10.5121/ijcsit.2012.4103. URL <http://dx.doi.org/10.5121/ijcsit.2012.4103>.
- N. Ravi, V. Gabeur, Y.-T. Hu, R. Hu, C. Ryali, T. Ma, H. Khedr, R. Rädle, C. Rolland, L. Gustafson, E. Mintun, J. Pan, K. V. Alwala, N. Carion, C.-Y. Wu, R. Girshick, P. Dollár, and C. Feichtenhofer. Sam 2: Segment anything in images and videos, 2024. URL <https://arxiv.org/abs/2408.00714>.
- A. Srinivas, M. Laskin, and P. Abbeel. Curl: Contrastive unsupervised representations for reinforcement learning, 2020. URL <https://arxiv.org/abs/2004.04136>.
- A. Paszke, S. Gross, F. Massa, A. Lerer, J. Bradbury, G. Chanan, T. Killeen, Z. Lin, N. Gimelshein, L. Antiga, A. Desmaison, A. Köpf, E. Yang, Z. DeVito, M. Raison, A. Tejani, S. Chilamkurthy, B. Steiner, L. Fang, J. Bai, and S. Chintala. Pytorch: An imperative style, high-performance deep learning library, 2019. URL <https://arxiv.org/abs/1912.01703>.
- A. Bou, M. Bettini, S. Dittert, V. Kumar, S. Sodhani, X. Yang, G. D. Fabritiis, and V. Moens. Torchrl: A data-driven decision-making library for pytorch, 2023. URL <https://arxiv.org/abs/2306.00577>.
- M. M. Krell, M. Kosec, S. P. Perez, and A. Fitzgibbon. Efficient sequence packing without cross-contamination: Accelerating large language models without impacting performance, 2022. URL <https://arxiv.org/abs/2107.02027>.

---

## Appendix

### A Visual Generalization Benchmark

#### A.1 Visual Perturbation Categories

Category	Perturbations
Camera	camera pose, camera FOV
Lighting	lighting direction, lighting color
Color	MO color, RO color, table color, ground color
Texture	MO texture, RO texture, table texture, ground texture

Table 1: Perturbation categories and their corresponding visual perturbation tests.

Table 1 lists the visual perturbation categories used in Figure 8.

#### A.2 Model Selection

For all methods, we tested the final model (for each seed) after 1 million training steps. Early stopping had no significant effect on results, so using the final checkpoint ensured consistency and simplicity across tests.

#### A.3 Scores Aggregation

Scores are computed using normalized returns, where each return is divided by the maximum number of steps for the task, yielding values in  $[0, 1]$ . To compute benchmark returns, we first evaluate baseline performance on the unperturbed tasks by running 50 rollouts per task and per model seed. Each average return (over 50 rollouts) is computed for all  $m = 8$  tasks and  $n = 5$  seeds, yielding  $m \times n = 40$  scores. We then compute the IQM and 95% confidence intervals using stratified bootstrap with 50,000 replications, following Agarwal et al. (2022).

For individual perturbation results (e.g., Table 3), we set  $m = 1$  (a single task) and  $n = 5$  (seeds), with each score averaged over 50 rollouts. For category-level scores (e.g., Camera Easy, Lighting Easy),  $m$  is the total number of perturbation-task combinations in that category. For instance, both the Camera and Lighting categories include two perturbations (Pose/FOV and Direction/Color, respectively) applied to 8 tasks, resulting in  $m = 2 \times 8 = 16$ .

Some perturbation categories involve a receiving object (RO), such as RO Texture and RO Color in the Texture and Color categories. Tasks that do not include a RO (e.g., LiftPegUpright) cannot be evaluated on these specific perturbations, reducing  $m$  by one for those tasks. As a result, the total number of perturbation-task pairs varies across categories depending on RO availability. For both Texture and Color, we obtain  $m = 29$  after summing over all tasks while accounting for the presence or absence of ROs. A summary of the number of valid perturbation-task pairs per category, accounting for RO presence, is shown in Table 2.

For the overall scores, we aggregated results across all tasks and all perturbations for each difficulty level, yielding a total of  $80 + 80 + 145 + 145 = 450$  test cases per difficulty. We then computed the IQM over these 450 results, providing a robust and reliable evaluation.

Perturbation Category	# Tests ( $m \times n$ )
Camera	$16 \times 5 = 80$
Lighting	$16 \times 5 = 80$
Color	$29 \times 5 = 145$
Texture	$29 \times 5 = 145$

Table 2: Number of test scores per visual perturbation category.

#### A.4 Difficulty Textures Examples

To illustrate the impact of benchmark difficulty on scene appearance, we include Blender renders of selected visual perturbations and full-scene previews for each task. Not all Blender renders are shown, the complete set is available at <https://segdac.github.io/>. The textures and colors are also task-specific, for example, in the Pick Cube task, the default cube is red and the target is green. Accordingly, the texture perturbations vary in difficulty: the easy texture resembles metallic red (similar to the default), the medium texture is unrelated to either red or green, and the hard texture uses green dots resembling the target to induce confusion.

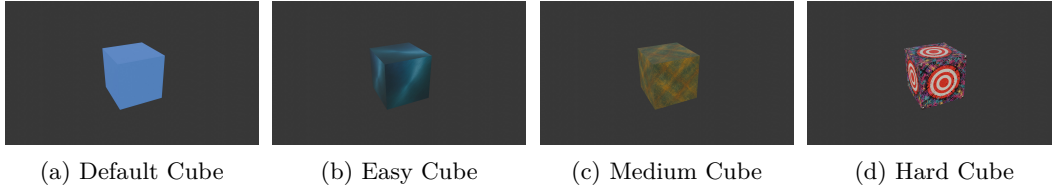


Figure 11: Blender renders for the cube, used in tasks like push/pull/poke cube.

Figure 11 shows how cube appearance changes with perturbation difficulty. The default cube (used when no perturbations are applied) is a solid light blue. The easy texture remains blue with minor variations, such as darker shades and simple patterns, maintaining high visual similarity with the default cube. The medium texture introduces green and yellow-brown tones with slightly more complex patterns, it does not share a lot (if any) visual similarity with the default cube while avoiding conflicts with other scene elements (e.g: robot arm, table, or target). The hard texture is visually and semantically disruptive: it features a chaotic mix of colors and complex patterns, with each cube face displaying a target identical to the task’s actual target. This creates a semantic clash, making it harder for the policy to recognize the cube. These examples demonstrate that our difficulty levels correspond to meaningful and progressively more challenging visual changes.

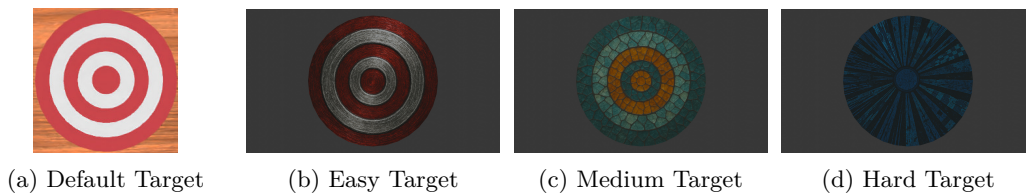


Figure 12: Blender renders for the target.

Figure 12 illustrates the different target textures across difficulty levels. The easy texture closely resembles the default, with red and white nested rings and a slight metallic finish to introduce subtle variation. The medium texture uses entirely different colors and more complex patterns, but retains the same nested ring structure and number of rings. The hard texture is significantly different: it replaces the nested rings with inward-pointing stripes,

---

resembling a dartboard. The color scheme also changes drastically (e.g., blue instead of red), making the target visually and semantically harder to recognize.

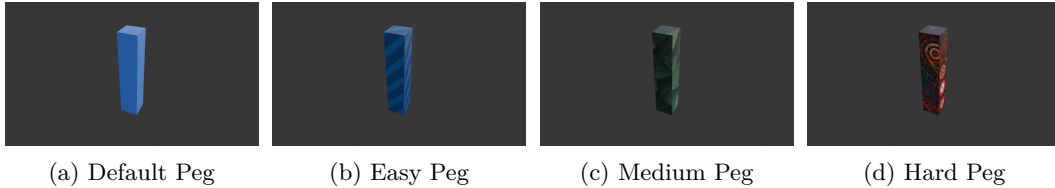


Figure 13: Blender renders for the peg used in the poke cube task.

Figure 13 shows the peg textures across difficulty levels. While multiple tasks include a peg, their textures may differ, the renders shown here are for the poke cube task. The easy texture shares strong visual similarity with the default view, as both are blue. The medium texture uses green, a neutral color that does not resemble any other object in the scene, and features a more complex pattern. The hard texture is visually and semantically distinct, with no similarity to the default. It includes repeated target symbols similar to those used for the task, increasing ambiguity and making the object harder to identify correctly.

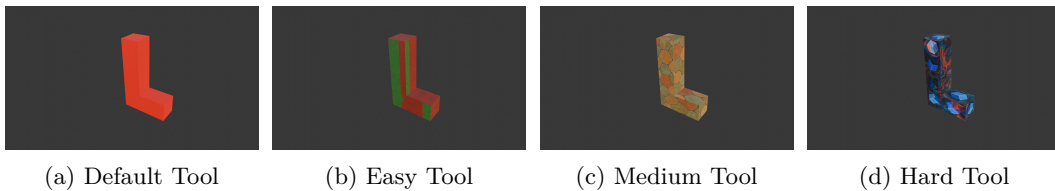


Figure 14: Blender renders for the l-shaped tool used in the pull cube tool task.

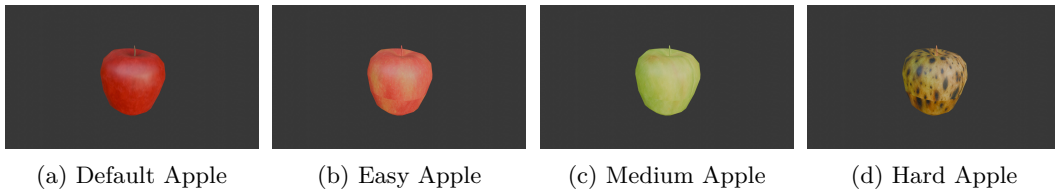


Figure 15: Blender renders for the apple used in the place apple in the bowl task.

Figure 15 shows the apple textures across difficulty levels. The default apple is a simple red apple. The easy texture is a lighter red with faint orange areas, maintaining strong visual similarity. The medium texture is green, representing a common apple variety, but differing in color. The hard texture shows a brownish, rotten apple that is both visually distinct and semantically less typical, representing a rare case that may be underrepresented in real-world data or training distributions.

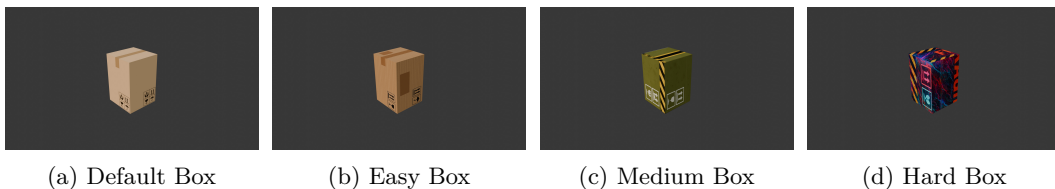


Figure 16: Blender renders for the box used in the transport box task.

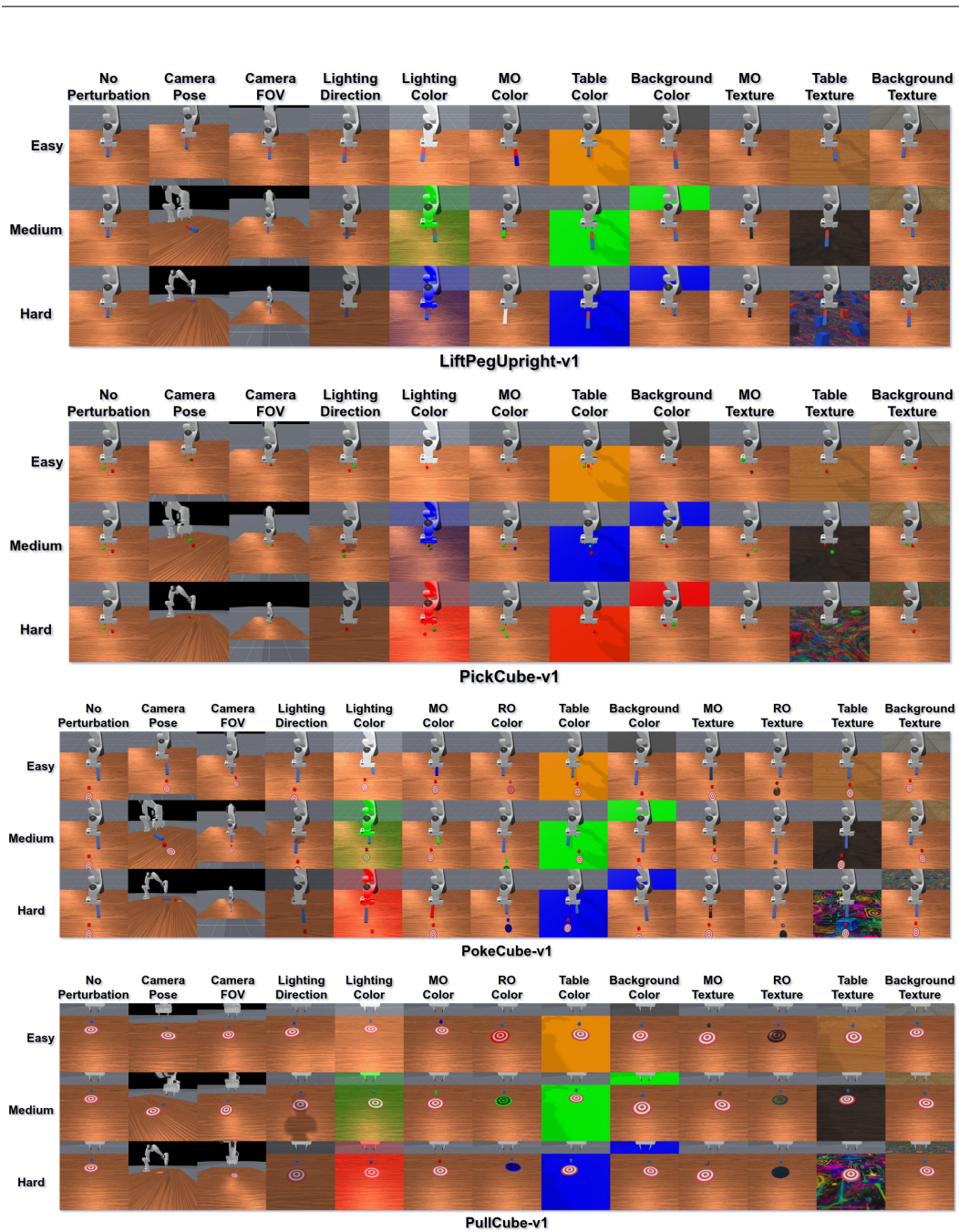


Figure 17: (Part 1) Visual perturbations for all tasks and difficulties.

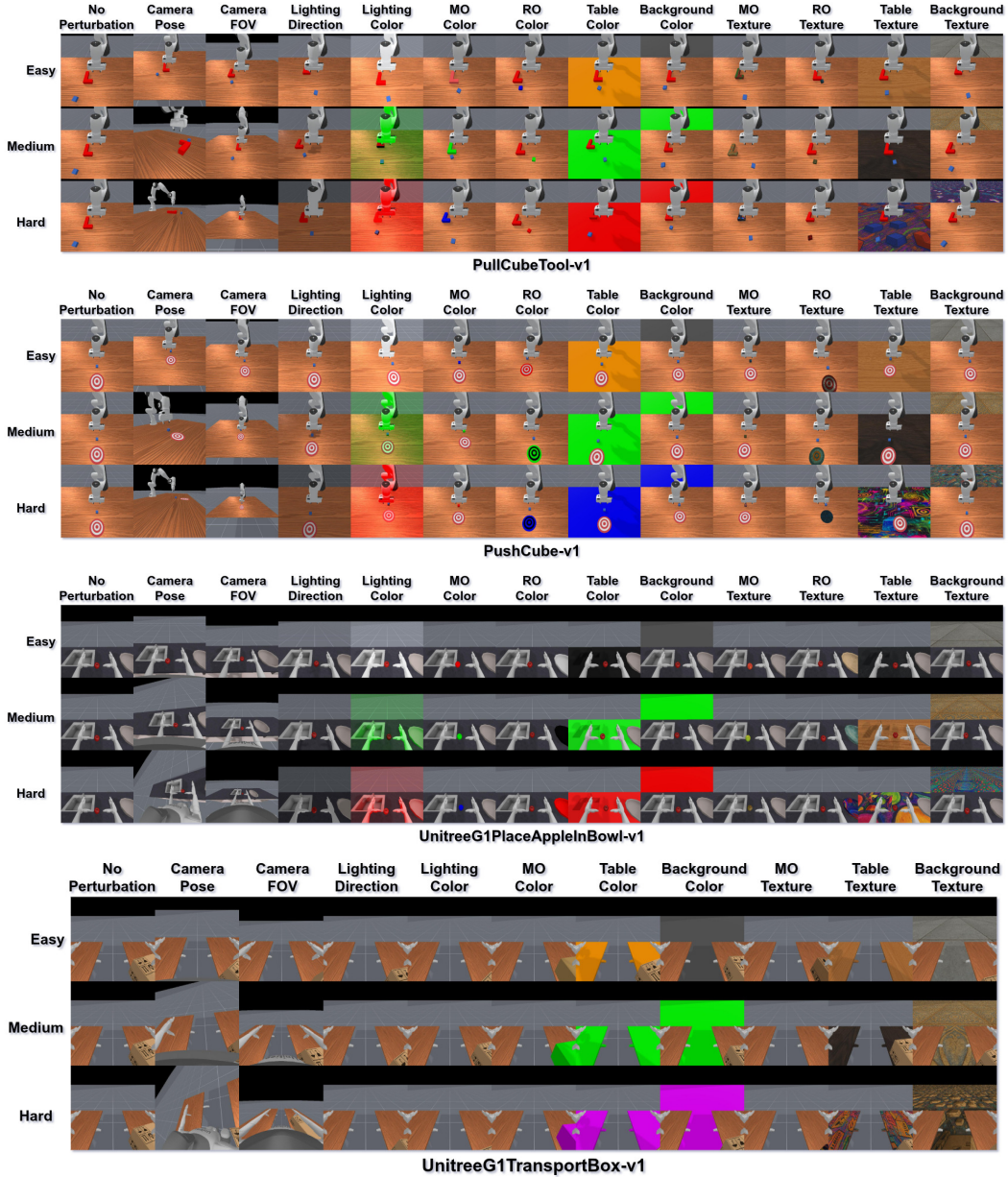


Figure 18: (Part 2) Visual perturbations for all tasks and difficulties.

Figures 17 and 18 show all visual perturbations for each task alongside their default (unperturbed) views. As difficulty increases, observations become more out-of-distribution and challenging. Notably, our camera pose perturbations are more aggressive than those typically used in other benchmarks, making them especially difficult for policies to handle. While no benchmark is perfect, we believe that exposing policies to strong perturbations provides a clearer understanding of their true robustness and generalization capabilities.

### A.5 Case Study & Failure Cases

Below are qualitative rollout examples comparing SegDAC to MaDi across various tasks and perturbations. We also include cases with camera pose perturbations, as they were the most challenging for all methods.

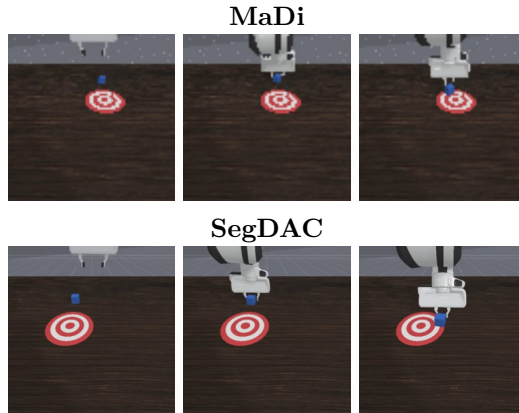


Figure 19: Rollout for *PullCube* - Medium Table Texture (top: MaDi, bottom: SegDAC).

Figure 19 shows that both MaDi and SegDAC are able to successfully complete the Pull Cube task under the medium table texture perturbation (success is reaching the first white ring), regardless of the target’s initial position. This highlights that, in some cases, policies can still succeed under medium-level perturbations and do not always collapse when faced with moderate visual changes.

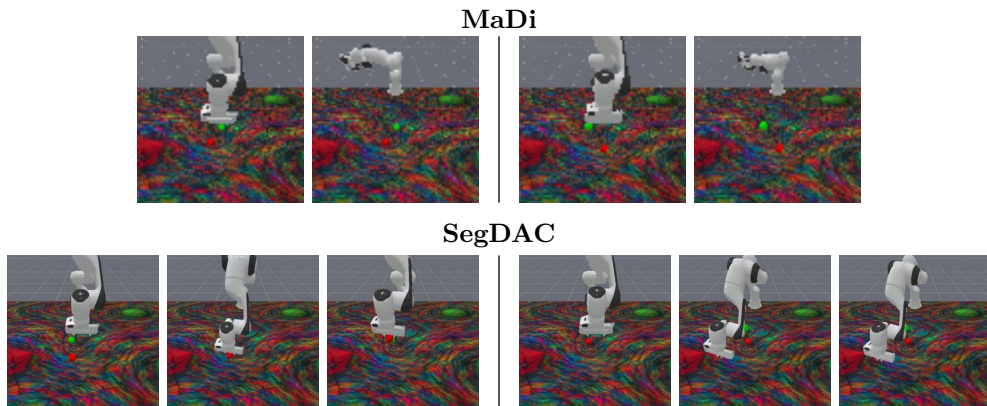


Figure 20: 2 Rollouts for *PickCube* - Hard Table Texture (top: MaDi, bottom: SegDAC).

Figure 20 shows the Pick Cube task under the challenging hard table texture, which includes complex patterns along with a red cube and green target embedded in the texture. This creates significant ambiguity, as the policy may confuse the textured cube with the actual object. MaDi consistently fails, often producing extreme and unstable actions. In contrast, SegDAC succeeds in some rollouts and fails in others. Its failures are more controlled, typically resulting from missed grasp attempts rather than erratic behavior.

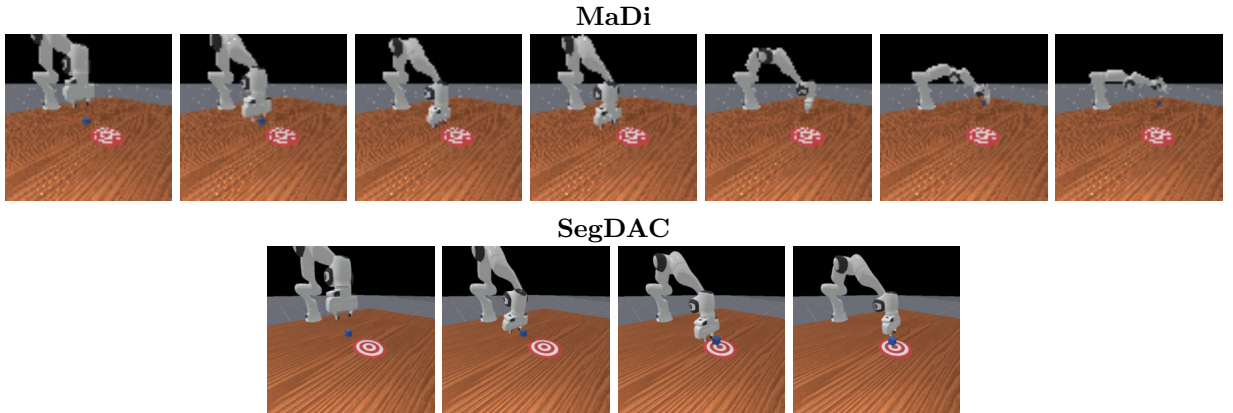


Figure 21: Rollout for *PushCube* - Medium Camera Pose (top: MaDi, bottom: SegDAC).

Figure 21 shows a rollout of the Push Cube task under the medium camera pose perturbation for both MaDi and SegDAC. MaDi initially behaves reasonably by reaching toward the cube, but fails to position the arm correctly. This leads to accumulating errors and eventually to unstable actions that push the cube away from the target. In contrast, SegDAC handles the perturbation more effectively and often succeeds, showing more stable and goal-directed behavior.

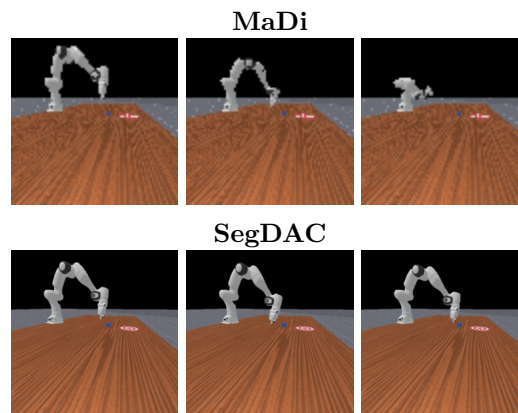


Figure 22: Rollout for *PushCube* - Hard Camera Pose (top: MaDi, bottom: SegDAC).

Figure 22 illustrates the difficulty of the hard camera pose perturbation for both policies. MaDi consistently collapses and produces erratic, non-sensical actions. While SegDAC does not succeed either, it shows more structured behavior, making small back-and-forth motions in an attempt to push the cube. However, it lacks the precision needed and repeatedly misses the cube by a small margin.

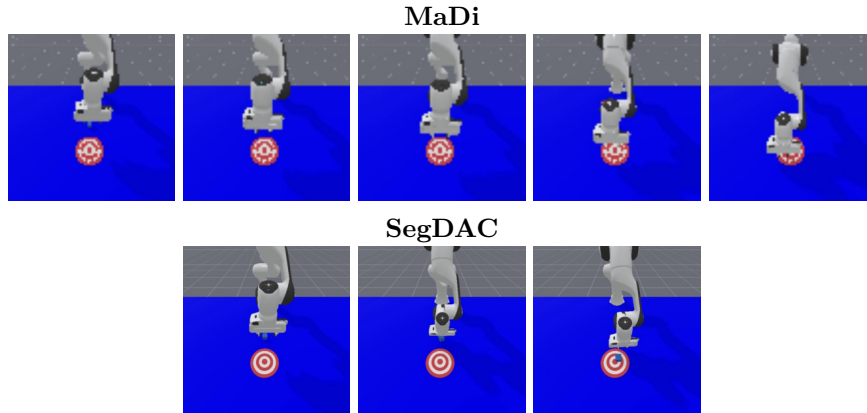


Figure 23: Rollout for *PushCube* - Hard Table Color (top: MaDi, bottom: SegDAC).

Figure 23 shows a rollout of the Push Cube task under the hard table color perturbation. In this case, the table is blue, the same color as the cube, which appears to confuse MaDi. The policy behaves as if the cube is already between the gripper and moves toward the target, while the actual cube remains at its initial position. This issue does not occur with SegDAC, which accurately identifies the cube and pushes it to the center of the target. This highlights the strength of object-centric approaches. While MaDi reasons at the pixel level, SegDAC decomposes the scene into segments and leverages bounding box coordinates of the cube segment to guide the policy more effectively.

## A.6 Exhaustive Results

Table 3 and the subsequent tables report IQM returns and 95% confidence intervals for each visual perturbation, across all tasks, methods, and difficulty levels. The method with the highest absolute IQM return is shown in **bold**, while the method with the best relative improvement over its no-perturbation baseline is underlined. We also include the relative delta between the baseline (no perturbation) IQM return and the return under the perturbed setting. For example, a value of (-2.5%) indicates a 2.5% performance drop compared to the no perturbation case.

Table 3: Easy Camera Fov Test

Task	SAC AE	DrQ-v2	MaDi	SADA	SegDAC
LiftPegUpright	0.20±0.00 (-7.8%)	0.23±0.09 (-50.3%)	0.22±0.01 (-0.3%)	0.22±0.01 (-1.1%)	<b>0.27±0.08 (-34.4%)</b>
PickCube	0.07±0.01 (-60.1%)	0.12±0.04 (-74.0%)	0.14±0.04 (-68.9%)	<b>0.26±0.08 (-32.0%)</b>	0.21±0.02 (-36.5%)
PokeCube	0.06±0.02 (-60.8%)	0.15±0.03 (-66.2%)	0.11±0.01 (-72.9%)	0.14±0.01 (-63.4%)	<b>0.18±0.01 (-55.0%)</b>
PullCube	0.09±0.03 (-76.5%)	0.09±0.06 (-76.0%)	<b>0.42±0.17 (-15.6%)</b>	<b>0.42±0.14 (-13.6%)</b>	0.32±0.12 (-35.7%)
PullCubeTool	0.05±0.03 (-76.8%)	0.12±0.20 (-80.6%)	0.21±0.03 (-65.9%)	0.26±0.10 (-28.3%)	<b>0.63±0.13 (-14.2%)</b>
PushCube	0.12±0.03 (-59.0%)	0.17±0.04 (-62.6%)	0.16±0.02 (-65.3%)	0.24±0.04 (-47.5%)	<b>0.59±0.10 (+30.3%)</b>
PlaceAppleInBowl	0.04±0.01 (-52.5%)	0.11±0.05 (-32.6%)	0.09±0.04 (-29.3%)	0.10±0.04 (-14.2%)	<b>0.21±0.11 (-32.8%)</b>
TransportBox	0.03±0.02 (-31.8%)	0.26±0.07 (-0.7%)	0.26±0.01 (-0.3%)	0.22±0.10 (-9.7%)	<b>0.27±0.01 (-2.5%)</b>

Table 4: Easy Camera Pose Test

Task	SAC AE	DrQ-v2	MaDi	SADA	SegDAC
LiftPegUpright	0.19±0.00 (-11.9%)	<b>0.23±0.09 (-50.5%)</b>	0.20±0.02 (-9.1%)	0.22±0.04 (-1.9%)	0.19±0.00 (-54.0%)
PickCube	0.05±0.02 (-74.9%)	0.07±0.10 (-85.2%)	<b>0.27±0.09 (-39.5%)</b>	0.25±0.06 (-34.5%)	0.12±0.05 (-65.5%)
PokeCube	0.03±0.01 (-83.8%)	0.02±0.01 (-94.6%)	0.16±0.01 (-60.2%)	<b>0.22±0.04 (-42.1%)</b>	0.13±0.02 (-66.7%)
PullCube	0.05±0.03 (-86.1%)	0.02±0.02 (-94.2%)	0.24±0.02 (-51.2%)	0.24±0.05 (-50.1%)	<b>0.35±0.13 (-30.4%)</b>
PullCubeTool	0.02±0.02 (-88.7%)	0.15±0.07 (-76.4%)	0.20±0.05 (-67.6%)	0.22±0.04 (-39.5%)	<b>0.59±0.18 (-20.7%)</b>
PushCube	0.06±0.05 (-80.1%)	0.08±0.06 (-81.4%)	0.30±0.09 (-36.0%)	<b>0.36±0.04 (-21.5%)</b>	0.10±0.11 (-77.3%)
PlaceAppleInBowl	0.03±0.02 (-59.1%)	0.15±0.02 (-11.3%)	0.12±0.06 (-3.5%)	0.12±0.04 (-2.4%)	<b>0.22±0.08 (-29.7%)</b>
TransportBox	0.04±0.04 (-12.6%)	0.26±0.07 (-1.2%)	0.26±0.02 (-0.5%)	0.22±0.10 (-10.5%)	<b>0.28±0.01 (-1.3%)</b>

Table 5: Easy Ground Color Test

Task	SAC AE	DrQ-v2	MaDi	SADA	SegDAC
LiftPegUpright	0.21±0.00 (-0.7%)	0.36±0.12 (-23.0%)	0.23±0.01 (+2.5%)	0.22±0.03 (+0.4%)	<b>0.39±0.15 (-5.5%)</b>
PickCube	0.12±0.01 (-33.7%)	0.13±0.09 (-72.5%)	<b>0.43±0.06 (-2.4%)</b>	0.41±0.03 (+4.7%)	0.35±0.04 (+3.1%)
PokeCube	0.16±0.02 (-0.5%)	0.20±0.12 (-53.3%)	<b>0.41±0.01 (-0.1%)</b>	0.37±0.07 (-3.8%)	0.34±0.06 (-12.1%)
PullCube	0.23±0.04 (-38.7%)	0.13±0.10 (-63.6%)	0.46±0.06 (-6.8%)	0.45±0.18 (-8.5%)	<b>0.51±0.06 (+1.4%)</b>
PullCubeTool	0.19±0.05 (-12.2%)	0.36±0.35 (-42.6%)	0.61±0.20 (-1.4%)	0.36±0.14 (-1.8%)	<b>0.69±0.14 (-7.3%)</b>
PushCube	0.21±0.03 (-29.2%)	0.32±0.16 (-28.9%)	0.44±0.09 (-4.1%)	<b>0.46±0.02 (-0.1%)</b>	0.44±0.04 (-1.8%)
PlaceAppleInBowl	0.08±0.02 (+7.0%)	0.15±0.02 (-8.5%)	0.12±0.05 (+1.0%)	0.11±0.04 (-3.9%)	<b>0.29±0.15 (-9.7%)</b>
TransportBox	0.05±0.04 (+9.2%)	0.24±0.08 (-5.7%)	0.26±0.00 (+0.1%)	0.22±0.10 (-11.9%)	<b>0.28±0.01 (-0.1%)</b>

Table 6: Easy Ground Texture Test

Task	SAC AE	DrQ-v2	MaDi	SADA	SegDAC
LiftPegUpright	0.21±0.01 (-1.3%)	<b>0.46±0.18 (-2.8%)</b>	0.22±0.01 (+1.6%)	0.23±0.03 (+1.6%)	0.42±0.15 (+1.9%)
PickCube	0.10±0.04 (-45.5%)	<b>0.44±0.03 (-4.8%)</b>	0.43±0.06 (-1.9%)	0.40±0.03 (+3.8%)	0.35±0.05 (+5.2%)
PokeCube	0.15±0.02 (-10.8%)	<b>0.43±0.06 (-0.4%)</b>	0.41±0.01 (-1.1%)	0.37±0.07 (-3.9%)	0.40±0.05 (+0.8%)
PullCube	0.25±0.03 (-32.4%)	0.37±0.05 (-0.1%)	0.48±0.03 (-2.5%)	0.42±0.15 (-13.2%)	<b>0.53±0.06 (+4.9%)</b>
PullCubeTool	0.19±0.06 (-15.4%)	0.62±0.17 (-0.6%)	0.61±0.21 (-1.9%)	0.34±0.17 (-8.3%)	<b>0.74±0.16 (-0.6%)</b>
PushCube	0.21±0.03 (-30.1%)	0.34±0.22 (-24.6%)	<b>0.46±0.07 (+0.2%)</b>	0.45±0.01 (-1.8%)	<b>0.46±0.04 (+2.9%)</b>
PlaceAppleInBowl	0.07±0.02 (-3.9%)	0.05±0.04 (-66.8%)	0.12±0.04 (+0.2%)	0.12±0.05 (-2.7%)	<b>0.30±0.17 (-4.7%)</b>
TransportBox	0.03±0.04 (-41.3%)	0.26±0.07 (+1.1%)	0.26±0.00 (-0.0%)	0.21±0.10 (-13.1%)	<b>0.28±0.01 (-0.4%)</b>

Table 7: Easy Lighting Color Test

Task	SAC AE	DrQ-v2	MaDi	SADA	SegDAC
LiftPegUpright	0.21±0.01 (-0.6%)	0.21±0.02 (-54.6%)	0.22±0.02 (+2.3%)	0.21±0.01 (-4.2%)	<b>0.41±0.15 (+0.2%)</b>
PickCube	0.16±0.04 (-13.6%)	0.07±0.04 (-84.8%)	<b>0.43±0.06 (-3.0%)</b>	0.21±0.07 (-46.4%)	0.24±0.05 (-28.9%)
PokeCube	0.16±0.02 (-5.7%)	0.10±0.05 (-76.9%)	<b>0.41±0.01 (-0.8%)</b>	0.17±0.04 (-55.1%)	0.36±0.03 (-7.8%)
PullCube	0.30±0.04 (-19.7%)	0.09±0.05 (-76.1%)	0.49±0.05 (-1.0%)	0.44±0.14 (-9.0%)	<b>0.51±0.05 (+0.8%)</b>
PullCubeTool	0.24±0.07 (+8.2%)	0.09±0.07 (-85.9%)	0.61±0.19 (-2.2%)	0.19±0.10 (-47.4%)	<b>0.72±0.12 (-2.9%)</b>
PushCube	0.26±0.02 (-12.8%)	0.16±0.06 (-64.5%)	0.44±0.07 (-4.7%)	0.37±0.11 (-18.8%)	<b>0.48±0.02 (+5.8%)</b>
PlaceAppleInBowl	0.08±0.03 (+12.3%)	0.04±0.06 (-75.6%)	0.12±0.04 (-6.0%)	0.11±0.06 (-9.9%)	<b>0.32±0.17 (+0.0%)</b>
TransportBox	0.05±0.03 (+3.3%)	0.26±0.07 (-0.6%)	0.26±0.01 (+0.1%)	0.24±0.09 (-0.7%)	<b>0.28±0.01 (+0.0%)</b>

Table 8: Easy Lighting Direction Test

Task	SAC AE	DrQ-v2	MaDi	SADA	SegDAC
LiftPegUpright	0.21±0.01 (-0.2%)	<b>0.46±0.18 (-1.7%)</b>	0.23±0.02 (+2.5%)	0.22±0.03 (+0.9%)	0.40±0.15 (-2.6%)
PickCube	0.17±0.03 (-8.8%)	<b>0.42±0.04 (-8.4%)</b>	0.41±0.05 (-6.0%)	0.38±0.04 (-1.0%)	0.33±0.04 (-2.9%)
PokeCube	0.16±0.03 (-1.8%)	0.39±0.04 (-10.5%)	<b>0.41±0.02 (+0.8%)</b>	0.38±0.08 (-1.9%)	0.40±0.03 (+2.9%)
PullCube	0.17±0.01 (-54.7%)	0.26±0.05 (-30.3%)	0.54±0.07 (+9.6%)	<b>0.55±0.24 (+12.0%)</b>	0.52±0.09 (+4.0%)
PullCubeTool	0.19±0.06 (-11.0%)	0.37±0.22 (-40.4%)	0.62±0.21 (-1.2%)	0.33±0.14 (-9.4%)	<b>0.71±0.12 (-4.6%)</b>
PushCube	0.27±0.03 (-7.7%)	0.46±0.22 (-0.1%)	0.43±0.07 (-6.9%)	<b>0.48±0.02 (+4.7%)</b>	0.45±0.04 (+0.0%)
PlaceAppleInBowl	0.08±0.02 (+4.2%)	0.14±0.03 (-12.0%)	0.11±0.05 (-8.2%)	0.12±0.04 (+0.2%)	<b>0.32±0.17 (+1.7%)</b>
TransportBox	0.05±0.03 (+0.8%)	0.26±0.07 (-0.5%)	0.26±0.01 (+0.1%)	0.24±0.09 (-0.3%)	<b>0.28±0.01 (-0.1%)</b>

Table 9: Easy Mo Color Test

Task	SAC AE	DrQ-v2	MaDi	SADA	SegDAC
LiftPegUpright	0.21±0.01 (-1.3%)	0.27±0.09 (-42.1%)	0.22±0.01 (-0.1%)	0.22±0.02 (-0.8%)	<b>0.40±0.15 (-2.5%)</b>
PickCube	0.14±0.03 (-22.0%)	0.25±0.06 (-45.0%)	<b>0.43±0.06 (-2.9%)</b>	0.31±0.06 (-20.1%)	0.28±0.06 (-17.4%)
PokeCube	0.13±0.02 (-24.1%)	0.17±0.01 (-60.0%)	0.39±0.01 (-4.4%)	0.30±0.05 (-22.1%)	<b>0.40±0.03 (+2.2%)</b>
PullCube	0.24±0.04 (-34.2%)	0.22±0.02 (-39.7%)	0.45±0.02 (-7.6%)	0.34±0.12 (-31.3%)	<b>0.48±0.08 (-3.7%)</b>
PullCubeTool	0.14±0.02 (-38.2%)	0.26±0.16 (-58.9%)	0.50±0.15 (-19.1%)	0.31±0.13 (-14.2%)	<b>0.81±0.17 (+9.8%)</b>
PushCube	0.20±0.03 (-32.0%)	0.23±0.16 (-48.7%)	0.43±0.07 (-6.4%)	0.33±0.13 (-29.1%)	<b>0.45±0.05 (-0.2%)</b>
PlaceAppleInBowl	0.07±0.01 (-7.7%)	0.08±0.04 (-53.4%)	0.13±0.04 (+4.5%)	0.09±0.04 (-21.7%)	<b>0.32±0.17 (+1.0%)</b>
TransportBox	0.05±0.03 (-1.0%)	0.26±0.07 (-0.6%)	0.26±0.01 (-0.0%)	0.24±0.09 (-2.2%)	<b>0.28±0.01 (-0.4%)</b>

Table 10: Easy Mo Texture Test

Task	SAC AE	DrQ-v2	MaDi	SADA	SegDAC
LiftPegUpright	0.20±0.01 (-5.7%)	0.22±0.02 (-52.8%)	0.20±0.01 (-6.8%)	0.22±0.02 (-2.6%)	<b>0.31±0.09 (-23.8%)</b>
PickCube	0.14±0.01 (-22.9%)	<b>0.24±0.05 (-48.0%)</b>	0.23±0.08 (-46.6%)	0.17±0.05 (-57.3%)	0.16±0.02 (-50.9%)
PokeCube	0.12±0.01 (-25.2%)	0.17±0.04 (-61.8%)	<b>0.38±0.03 (-8.1%)</b>	0.22±0.03 (-42.3%)	0.36±0.03 (-8.2%)
PullCube	0.25±0.03 (-32.6%)	0.27±0.05 (-27.1%)	<b>0.47±0.05 (-5.1%)</b>	0.37±0.02 (-24.3%)	0.46±0.10 (-8.5%)
PullCubeTool	0.13±0.05 (-42.0%)	0.12±0.07 (-80.5%)	0.23±0.08 (-63.7%)	0.11±0.14 (-68.9%)	<b>0.35±0.08 (-53.1%)</b>
PushCube	0.18±0.02 (-38.9%)	0.18±0.10 (-59.5%)	0.22±0.16 (-51.9%)	0.19±0.04 (-57.9%)	<b>0.48±0.08 (+7.3%)</b>
PlaceAppleInBowl	0.08±0.02 (+8.5%)	0.15±0.02 (-7.6%)	0.12±0.05 (-5.3%)	0.12±0.04 (-1.2%)	<b>0.29±0.17 (-8.2%)</b>
TransportBox	0.05±0.03 (+4.5%)	0.26±0.07 (-1.1%)	0.26±0.01 (+0.1%)	0.24±0.09 (-3.5%)	<b>0.28±0.01 (+0.0%)</b>

Table 11: Easy Ro Color Test

Task	SAC AE	DrQ-v2	MaDi	SADA	SegDAC
LiftPegUpright	N/A	N/A	N/A	N/A	N/A
PickCube	N/A	N/A	N/A	N/A	N/A
PokeCube	0.17±0.03 (+0.8%)	<b>0.42±0.05 (-3.7%)</b>	0.40±0.01 (-2.3%)	0.38±0.08 (-1.2%)	0.40±0.02 (+1.8%)
PullCube	0.34±0.06 (-8.7%)	0.29±0.08 (-20.3%)	0.50±0.05 (+1.1%)	0.41±0.11 (-16.6%)	<b>0.51±0.09 (+1.0%)</b>
PullCubeTool	0.18±0.06 (-15.4%)	0.48±0.21 (-22.4%)	0.60±0.18 (-3.5%)	0.30±0.16 (-18.6%)	<b>0.70±0.14 (-5.9%)</b>
PushCube	0.26±0.03 (-13.1%)	0.23±0.22 (-48.8%)	0.43±0.07 (-6.3%)	0.43±0.04 (-6.8%)	<b>0.44±0.04 (-2.9%)</b>
PlaceAppleInBowl	0.08±0.03 (+6.9%)	0.11±0.02 (-32.4%)	0.12±0.05 (-0.7%)	0.12±0.04 (+0.2%)	<b>0.29±0.14 (-7.0%)</b>
TransportBox	N/A	N/A	N/A	N/A	N/A

Table 12: Easy Ro Texture Test

Task	SAC AE	DrQ-v2	MaDi	SADA	SegDAC
LiftPegUpright	N/A	N/A	N/A	N/A	N/A
PickCube	N/A	N/A	N/A	N/A	N/A
PokeCube	0.17±0.04 (+0.9%)	0.35±0.04 (-19.5%)	<b>0.41±0.01 (-0.0%)</b>	0.38±0.07 (-2.1%)	0.40±0.04 (+2.0%)
PullCube	0.35±0.03 (-6.0%)	0.14±0.12 (-63.0%)	0.58±0.07 (+17.4%)	<b>0.70±0.05 (+43.4%)</b>	0.55±0.07 (+9.1%)
PullCubeTool	0.20±0.07 (-6.8%)	0.57±0.26 (-8.2%)	0.63±0.20 (+1.2%)	0.35±0.13 (-3.6%)	<b>0.72±0.12 (-2.3%)</b>
PushCube	0.24±0.03 (-19.4%)	0.33±0.23 (-28.4%)	0.56±0.13 (+19.8%)	<b>0.57±0.07 (+22.9%)</b>	0.49±0.05 (+10.0%)
PlaceAppleInBowl	0.06±0.02 (-20.5%)	0.06±0.04 (-63.9%)	0.12±0.05 (-3.2%)	0.11±0.04 (-3.2%)	<b>0.23±0.12 (-25.7%)</b>
TransportBox	N/A	N/A	N/A	N/A	N/A

Table 13: Easy Table Color Test

Task	SAC AE	DrQ-v2	MaDi	SADA	SegDAC
LiftPegUpright	0.21±0.00 (-2.3%)	0.21±0.02 (-55.3%)	0.21±0.01 (-6.2%)	0.22±0.03 (-1.3%)	<b>0.28±0.08 (-32.2%)</b>
PickCube	0.06±0.05 (-68.1%)	0.05±0.11 (-88.7%)	<b>0.43±0.06 (-2.1%)</b>	0.26±0.07 (-32.7%)	0.19±0.04 (-43.0%)
PokeCube	0.14±0.02 (-16.5%)	0.30±0.14 (-32.1%)	<b>0.40±0.01 (-3.5%)</b>	0.28±0.07 (-28.4%)	0.24±0.02 (-38.6%)
PullCube	0.14±0.07 (-63.2%)	0.30±0.22 (-18.0%)	0.39±0.14 (-21.6%)	<b>0.42±0.03 (-13.3%)</b>	<b>0.42±0.05 (-15.7%)</b>
PullCubeTool	0.19±0.06 (-14.6%)	<b>0.61±0.17 (-1.4%)</b>	0.43±0.28 (-31.6%)	0.35±0.18 (-5.1%)	0.48±0.12 (-35.4%)
PushCube	0.24±0.06 (-19.2%)	0.39±0.25 (-14.8%)	0.45±0.08 (-2.2%)	0.45±0.05 (-3.4%)	<b>0.66±0.08 (+46.3%)</b>
PlaceAppleInBowl	0.06±0.04 (-13.1%)	0.09±0.04 (-44.1%)	0.12±0.06 (-6.3%)	0.10±0.05 (-15.9%)	<b>0.30±0.16 (-5.0%)</b>
TransportBox	0.06±0.03 (+17.4%)	0.19±0.11 (-25.8%)	0.26±0.00 (-0.2%)	0.24±0.09 (-3.7%)	<b>0.28±0.01 (-0.5%)</b>

Table 14: Easy Table Texture Test

Task	SAC AE	DrQ-v2	MaDi	SADA	SegDAC
LiftPegUpright	0.21±0.00 (+0.2%)	<b>0.40±0.19 (-15.7%)</b>	0.23±0.01 (+2.5%)	0.22±0.05 (+0.6%)	0.39±0.13 (-5.4%)
PickCube	0.16±0.07 (-13.8%)	0.33±0.15 (-27.8%)	<b>0.42±0.05 (-5.1%)</b>	0.35±0.07 (-9.3%)	0.34±0.03 (+1.5%)
PokeCube	0.16±0.01 (-5.3%)	0.40±0.05 (-6.9%)	<b>0.41±0.02 (+0.1%)</b>	0.36±0.08 (-6.9%)	0.38±0.01 (-2.7%)
PullCube	0.33±0.04 (-10.9%)	0.37±0.03 (+1.1%)	0.49±0.05 (+0.3%)	<b>0.50±0.12 (+2.3%)</b>	<b>0.50±0.08 (-0.8%)</b>
PullCubeTool	0.22±0.07 (-1.4%)	0.41±0.24 (-33.8%)	0.60±0.20 (-4.0%)	0.29±0.08 (-20.8%)	<b>0.61±0.18 (-17.2%)</b>
PushCube	0.26±0.05 (-11.7%)	0.45±0.23 (-2.0%)	0.45±0.06 (-2.6%)	0.45±0.09 (-3.2%)	<b>0.48±0.06 (+6.9%)</b>
PlaceAppleInBowl	0.07±0.02 (-0.8%)	0.13±0.02 (-22.5%)	0.11±0.07 (-7.6%)	0.10±0.04 (-14.3%)	<b>0.28±0.16 (-10.0%)</b>
TransportBox	0.06±0.04 (+27.8%)	0.24±0.07 (-6.9%)	0.26±0.00 (-0.8%)	0.24±0.09 (-1.3%)	<b>0.28±0.01 (-0.3%)</b>

Table 15: Medium Camera Fov Test

Task	SAC AE	DrQ-v2	MaDi	SADA	SegDAC
LiftPegUpright	0.19±0.00 (-11.7%)	0.19±0.01 (-59.3%)	0.21±0.00 (-5.5%)	0.21±0.01 (-3.6%)	<b>0.22±0.00 (-47.6%)</b>
PickCube	0.02±0.02 (-88.9%)	0.02±0.01 (-96.7%)	0.08±0.02 (-82.8%)	<b>0.11±0.02 (-71.7%)</b>	0.06±0.02 (-81.7%)
PokeCube	0.01±0.01 (-92.3%)	0.02±0.01 (-95.8%)	0.09±0.02 (-78.7%)	<b>0.11±0.02 (-71.6%)</b>	0.09±0.01 (-75.8%)
PullCube	0.05±0.02 (-86.9%)	0.03±0.02 (-92.8%)	0.15±0.03 (-69.0%)	<b>0.19±0.03 (-60.1%)</b>	0.18±0.02 (-64.9%)
PullCubeTool	0.02±0.01 (-90.0%)	0.03±0.05 (-95.2%)	0.10±0.02 (-83.2%)	0.15±0.05 (-58.7%)	<b>0.30±0.10 (-59.3%)</b>
PushCube	0.02±0.02 (-91.7%)	0.02±0.01 (-96.4%)	0.06±0.02 (-87.5%)	<b>0.16±0.03 (-65.4%)</b>	0.08±0.03 (-82.6%)
PlaceAppleInBowl	0.01±0.01 (-80.9%)	<b>0.03±0.01 (-82.1%)</b>	<b>0.03±0.02 (-77.5%)</b>	<b>0.03±0.04 (-71.5%)</b>	<b>0.03±0.04 (-89.6%)</b>
TransportBox	0.03±0.03 (-32.9%)	0.18±0.07 (-31.8%)	0.20±0.06 (-21.8%)	0.16±0.08 (-33.6%)	<b>0.27±0.01 (-1.8%)</b>

Table 16: Medium Camera Pose Test

Task	SAC AE	DrQ-v2	MaDi	SADA	SegDAC
LiftPegUpright	0.19±0.01 (-10.9%)	0.19±0.01 (-59.0%)	0.20±0.02 (-10.1%)	0.19±0.01 (-13.3%)	<b>0.23±0.01 (-45.3%)</b>
PickCube	0.03±0.01 (-84.4%)	0.03±0.01 (-94.5%)	0.07±0.02 (-84.8%)	0.11±0.02 (-71.8%)	<b>0.12±0.04 (-64.7%)</b>
PokeCube	0.02±0.02 (-86.4%)	0.02±0.03 (-95.9%)	0.08±0.02 (-79.6%)	<b>0.11±0.02 (-72.8%)</b>	0.10±0.01 (-74.6%)
PullCube	0.04±0.01 (-90.5%)	0.02±0.02 (-95.9%)	0.06±0.03 (-87.5%)	<b>0.16±0.04 (-66.9%)</b>	0.07±0.02 (-85.4%)
PullCubeTool	0.02±0.02 (-91.1%)	0.01±0.01 (-99.1%)	0.01±0.01 (-98.8%)	<b>0.03±0.01 (-93.1%)</b>	0.01±0.01 (-98.4%)
PushCube	0.04±0.01 (-85.6%)	0.02±0.01 (-94.8%)	0.10±0.01 (-78.6%)	0.10±0.03 (-78.8%)	<b>0.34±0.06 (-24.7%)</b>
PlaceAppleInBowl	0.01±0.01 (-86.5%)	0.05±0.03 (-70.6%)	0.03±0.02 (-77.6%)	<b>0.08±0.06 (-34.5%)</b>	0.05±0.08 (-84.3%)
TransportBox	0.04±0.03 (-29.4%)	0.06±0.02 (-75.9%)	0.10±0.06 (-61.8%)	0.14±0.08 (-44.7%)	<b>0.27±0.02 (-3.2%)</b>

Table 17: Medium Ground Color Test

Task	SAC AE	DrQ-v2	MaDi	SADA	SegDAC
LiftPegUpright	0.21±0.00 (-1.1%)	0.21±0.02 (-55.3%)	0.22±0.02 (-0.9%)	0.21±0.04 (-3.0%)	<b>0.39±0.16 (-5.1%)</b>
PickCube	0.04±0.02 (-80.1%)	0.02±0.01 (-96.7%)	<b>0.43±0.06 (-1.5%)</b>	0.35±0.04 (-8.4%)	0.33±0.05 (-2.2%)
PokeCube	0.12±0.05 (-28.7%)	0.09±0.07 (-79.9%)	<b>0.41±0.02 (-0.3%)</b>	0.32±0.08 (-18.0%)	0.38±0.03 (-4.3%)
PullCube	0.18±0.05 (-50.9%)	0.02±0.08 (-95.7%)	0.34±0.14 (-30.1%)	0.33±0.10 (-31.7%)	<b>0.55±0.06 (+10.5%)</b>
PullCubeTool	0.16±0.08 (-25.4%)	0.09±0.12 (-85.4%)	0.47±0.16 (-24.6%)	0.29±0.07 (-20.5%)	<b>0.59±0.12 (-20.8%)</b>
PushCube	0.23±0.02 (-23.4%)	0.03±0.05 (-92.4%)	0.43±0.09 (-7.3%)	0.38±0.11 (-17.0%)	<b>0.47±0.03 (+4.0%)</b>
PlaceAppleInBowl	0.08±0.03 (+1.1%)	0.01±0.04 (-95.9%)	0.10±0.04 (-21.2%)	0.10±0.04 (-15.0%)	<b>0.30±0.16 (-4.4%)</b>
TransportBox	0.04±0.02 (-20.3%)	0.05±0.08 (-81.0%)	0.26±0.01 (-1.1%)	0.23±0.10 (-6.3%)	<b>0.28±0.01 (-0.1%)</b>

Table 18: Medium Ground Texture Test

Task	SAC AE	DrQ-v2	MaDi	SADA	SegDAC
LiftPegUpright	0.21±0.01 (-1.3%)	<b>0.42±0.18 (-10.7%)</b>	0.22±0.01 (-0.1%)	0.22±0.04 (+1.2%)	0.39±0.15 (-4.2%)
PickCube	0.07±0.01 (-59.5%)	0.39±0.03 (-15.8%)	<b>0.43±0.06 (-1.6%)</b>	0.36±0.04 (-6.7%)	0.33±0.03 (-3.1%)
PokeCube	0.13±0.02 (-22.4%)	<b>0.40±0.09 (-7.7%)</b>	<b>0.40±0.01 (-2.2%)</b>	0.25±0.09 (-36.3%)	0.39±0.02 (-1.5%)
PullCube	0.15±0.04 (-58.8%)	0.31±0.02 (-16.0%)	0.26±0.06 (-46.6%)	0.24±0.04 (-50.6%)	<b>0.51±0.06 (+1.6%)</b>
PullCubeTool	0.19±0.04 (-13.7%)	0.56±0.13 (-9.6%)	0.58±0.19 (-7.0%)	0.30±0.15 (-16.8%)	<b>0.72±0.14 (-3.3%)</b>
PushCube	0.14±0.03 (-53.3%)	0.43±0.22 (-6.7%)	0.44±0.08 (-4.4%)	0.33±0.08 (-27.7%)	<b>0.49±0.06 (+9.1%)</b>
PlaceAppleInBowl	0.01±0.01 (-87.4%)	0.00±0.01 (-97.4%)	0.06±0.05 (-47.2%)	0.10±0.04 (-15.8%)	<b>0.30±0.16 (-6.4%)</b>
TransportBox	0.04±0.04 (-26.2%)	0.11±0.10 (-58.6%)	0.11±0.06 (-58.4%)	0.09±0.05 (-62.5%)	<b>0.28±0.01 (-1.1%)</b>

Table 19: Medium Lighting Color Test

Task	SAC AE	DrQ-v2	MaDi	SADA	SegDAC
LiftPegUpright	0.21±0.00 (-2.0%)	0.19±0.00 (-60.2%)	0.22±0.01 (-0.6%)	0.23±0.03 (+2.5%)	<b>0.43±0.16 (+4.3%)</b>
PickCube	0.05±0.01 (-70.7%)	0.01±0.01 (-98.3%)	<b>0.19±0.02 (-56.1%)</b>	0.10±0.05 (-73.0%)	0.16±0.02 (-51.9%)
PokeCube	0.06±0.04 (-60.8%)	0.06±0.05 (-85.8%)	<b>0.38±0.03 (-8.3%)</b>	0.18±0.07 (-53.1%)	0.30±0.03 (-24.1%)
PullCube	0.20±0.06 (-47.0%)	0.05±0.03 (-86.8%)	0.37±0.05 (-24.0%)	0.29±0.11 (-41.4%)	<b>0.49±0.08 (-1.9%)</b>
PullCubeTool	0.12±0.04 (-45.6%)	0.06±0.03 (-90.4%)	0.15±0.12 (-76.3%)	0.32±0.15 (-12.5%)	<b>0.55±0.13 (-26.0%)</b>
PushCube	0.18±0.03 (-39.7%)	0.03±0.03 (-92.9%)	0.48±0.10 (+2.9%)	0.32±0.05 (-31.0%)	<b>0.53±0.06 (+18.1%)</b>
PlaceAppleInBowl	0.05±0.01 (-32.0%)	0.01±0.01 (-91.0%)	0.07±0.04 (-41.7%)	0.10±0.04 (-17.4%)	<b>0.28±0.14 (-11.2%)</b>
TransportBox	0.05±0.03 (+4.9%)	0.26±0.07 (-0.6%)	0.26±0.01 (-0.0%)	0.25±0.09 (+0.4%)	<b>0.28±0.01 (+0.4%)</b>

Table 20: Medium Lighting Direction Test

Task	SAC AE	DrQ-v2	MaDi	SADA	SegDAC
LiftPegUpright	0.21±0.01 (-0.6%)	0.23±0.03 (-51.0%)	0.21±0.01 (-2.4%)	0.22±0.04 (-0.6%)	<b>0.42±0.16 (+1.3%)</b>
PickCube	0.16±0.03 (-14.0%)	0.36±0.10 (-21.2%)	<b>0.43±0.05 (-2.7%)</b>	0.35±0.05 (-8.7%)	0.24±0.04 (-28.2%)
PokeCube	0.15±0.01 (-7.2%)	0.30±0.09 (-30.0%)	<b>0.41±0.02 (-0.3%)</b>	0.36±0.07 (-7.3%)	0.36±0.03 (-7.0%)
PullCube	0.28±0.01 (-24.2%)	0.34±0.10 (-6.8%)	0.49±0.03 (-1.3%)	0.49±0.07 (+1.4%)	<b>0.50±0.07 (+0.5%)</b>
PullCubeTool	0.22±0.06 (+1.4%)	0.47±0.20 (-25.1%)	0.58±0.20 (-6.3%)	0.30±0.10 (-18.7%)	<b>0.71±0.12 (-4.0%)</b>
PushCube	0.25±0.04 (-16.8%)	<b>0.51±0.24 (+12.7%)</b>	0.46±0.10 (-1.1%)	0.46±0.05 (-1.3%)	0.48±0.05 (+6.8%)
PlaceAppleInBowl	0.07±0.02 (+0.3%)	0.14±0.03 (-13.5%)	0.12±0.04 (+0.0%)	0.12±0.04 (+0.8%)	<b>0.29±0.15 (-7.3%)</b>
TransportBox	0.05±0.03 (+0.3%)	0.26±0.07 (-0.4%)	0.26±0.01 (-0.0%)	0.25±0.09 (+0.0%)	<b>0.28±0.01 (+0.2%)</b>

Table 21: Medium Mo Color Test

Task	SAC AE	DrQ-v2	MaDi	SADA	SegDAC
LiftPegUpright	0.20±0.01 (-5.4%)	0.23±0.04 (-51.3%)	0.21±0.01 (-4.8%)	0.22±0.01 (-0.2%)	<b>0.41±0.15 (-0.7%)</b>
PickCube	0.11±0.03 (-37.7%)	0.21±0.12 (-53.3%)	0.02±0.01 (-96.3%)	0.22±0.09 (-43.6%)	<b>0.27±0.05 (-18.8%)</b>
PokeCube	0.07±0.01 (-55.0%)	0.02±0.02 (-96.1%)	0.07±0.15 (-83.2%)	0.17±0.03 (-55.4%)	<b>0.40±0.04 (+1.5%)</b>
PullCube	0.15±0.05 (-60.0%)	0.08±0.02 (-77.8%)	0.10±0.06 (-79.1%)	0.46±0.12 (-5.4%)	<b>0.47±0.07 (-6.4%)</b>
PullCubeTool	0.09±0.02 (-59.0%)	0.03±0.04 (-94.8%)	0.12±0.05 (-80.1%)	0.25±0.17 (-30.6%)	<b>0.49±0.06 (-34.1%)</b>
PushCube	0.15±0.01 (-48.7%)	0.01±0.00 (-96.7%)	0.09±0.03 (-80.1%)	0.41±0.16 (-11.3%)	<b>0.47±0.03 (+4.7%)</b>
PlaceAppleInBowl	0.01±0.00 (-80.0%)	0.01±0.00 (-95.2%)	0.06±0.03 (-52.2%)	0.04±0.04 (-64.2%)	<b>0.29±0.16 (-8.3%)</b>
TransportBox	0.05±0.03 (-1.0%)	0.16±0.10 (-39.0%)	0.26±0.01 (-0.3%)	0.23±0.09 (-5.5%)	<b>0.28±0.01 (+0.3%)</b>

Table 22: Medium Mo Texture Test

Task	SAC AE	DrQ-v2	MaDi	SADA	SegDAC
LiftPegUpright	0.20±0.01 (-5.5%)	0.20±0.00 (-58.6%)	0.20±0.00 (-10.2%)	0.21±0.01 (-5.2%)	<b>0.30±0.09 (-27.5%)</b>
PickCube	0.05±0.02 (-71.1%)	0.01±0.00 (-97.3%)	0.01±0.00 (-98.1%)	0.02±0.02 (-94.3%)	<b>0.10±0.02 (-70.2%)</b>
PokeCube	0.08±0.01 (-52.4%)	0.07±0.02 (-84.4%)	0.16±0.10 (-60.8%)	0.06±0.02 (-85.6%)	<b>0.26±0.05 (-32.4%)</b>
PullCube	0.10±0.01 (-72.0%)	0.08±0.01 (-77.4%)	0.12±0.07 (-76.6%)	0.08±0.04 (-83.1%)	<b>0.47±0.07 (-6.8%)</b>
PullCubeTool	0.07±0.02 (-68.1%)	0.02±0.01 (-96.5%)	0.04±0.03 (-93.0%)	0.04±0.07 (-89.1%)	<b>0.20±0.08 (-73.1%)</b>
PushCube	0.11±0.03 (-62.1%)	0.02±0.00 (-96.5%)	0.10±0.04 (-78.9%)	0.06±0.02 (-86.8%)	<b>0.46±0.05 (+1.9%)</b>
PlaceAppleInBowl	0.03±0.01 (-60.1%)	0.04±0.02 (-78.1%)	0.04±0.02 (-67.8%)	0.03±0.03 (-73.4%)	<b>0.29±0.17 (-6.7%)</b>
TransportBox	0.05±0.04 (+4.1%)	0.25±0.08 (-4.9%)	0.26±0.01 (-0.0%)	0.23±0.09 (-5.4%)	<b>0.28±0.01 (-0.3%)</b>

Table 23: Medium Ro Color Test

Task	SAC AE	DrQ-v2	MaDi	SADA	SegDAC
LiftPegUpright	N/A	N/A	N/A	N/A	N/A
PickCube	N/A	N/A	N/A	N/A	N/A
PokeCube	0.16±0.02 (-5.1%)	0.30±0.06 (-30.2%)	<b>0.41±0.02 (-0.9%)</b>	0.36±0.07 (-8.0%)	0.38±0.03 (-3.0%)
PullCube	0.30±0.05 (-18.4%)	0.16±0.09 (-57.3%)	0.51±0.11 (+3.8%)	<b>0.53±0.19 (+9.2%)</b>	0.50±0.06 (+0.6%)
PullCubeTool	0.21±0.06 (-2.5%)	0.54±0.26 (-12.6%)	0.63±0.20 (+0.6%)	0.33±0.21 (-10.4%)	<b>0.70±0.11 (-5.1%)</b>
PushCube	0.25±0.03 (-14.7%)	0.35±0.23 (-24.3%)	<b>0.49±0.07 (+6.1%)</b>	0.45±0.10 (-2.2%)	0.45±0.05 (+0.4%)
PlaceAppleInBowl	<b>0.08±0.02 (+12.4%)</b>	0.14±0.03 (-17.0%)	0.11±0.05 (-6.7%)	0.12±0.04 (-2.9%)	<b>0.25±0.09 (-19.5%)</b>
TransportBox	N/A	N/A	N/A	N/A	N/A

Table 24: Medium Ro Texture Test

Task	SAC AE	DrQ-v2	MaDi	SADA	SegDAC
LiftPegUpright	N/A	N/A	N/A	N/A	N/A
PickCube	N/A	N/A	N/A	N/A	N/A
PokeCube	0.17±0.02 (+3.2%)	0.32±0.04 (-26.8%)	<b>0.41±0.01 (-1.0%)</b>	0.37±0.08 (-5.1%)	0.39±0.03 (-1.4%)
PullCube	0.35±0.04 (-6.4%)	0.09±0.08 (-75.1%)	0.43±0.09 (-12.3%)	<b>0.60±0.11 (+22.6%)</b>	0.51±0.06 (+2.6%)
PullCubeTool	0.20±0.07 (-9.9%)	0.50±0.23 (-18.8%)	0.67±0.19 (+7.2%)	0.33±0.17 (-10.8%)	<b>0.70±0.14 (-5.9%)</b>
PushCube	0.24±0.04 (-19.3%)	0.28±0.23 (-38.1%)	0.46±0.07 (-1.2%)	<b>0.52±0.08 (+13.6%)</b>	0.50±0.04 (+12.0%)
PlaceAppleInBowl	0.07±0.03 (-1.4%)	0.14±0.03 (-14.0%)	0.12±0.05 (+1.3%)	0.12±0.04 (+0.6%)	<b>0.22±0.12 (-29.0%)</b>
TransportBox	N/A	N/A	N/A	N/A	N/A

Table 25: Medium Table Color Test

Task	SAC AE	DrQ-v2	MaDi	SADA	SegDAC
LiftPegUpright	0.21±0.01 (-3.3%)	0.19±0.00 (-60.0%)	0.20±0.01 (-10.9%)	0.22±0.03 (+0.6%)	<b>0.38±0.13 (-6.7%)</b>
PickCube	0.04±0.00 (-79.6%)	0.00±0.00 (-99.1%)	0.06±0.04 (-85.6%)	0.08±0.02 (-80.0%)	<b>0.17±0.04 (-48.9%)</b>
PokeCube	0.08±0.03 (-53.4%)	0.05±0.05 (-89.3%)	0.23±0.12 (-44.9%)	<b>0.29±0.05 (-25.9%)</b>	0.28±0.02 (-28.4%)
PullCube	0.12±0.09 (-66.4%)	0.03±0.03 (-90.7%)	0.36±0.20 (-27.0%)	0.36±0.06 (-26.2%)	<b>0.42±0.06 (-15.9%)</b>
PullCubeTool	0.12±0.09 (-44.9%)	0.06±0.04 (-90.9%)	0.09±0.02 (-85.6%)	0.19±0.10 (-48.7%)	<b>0.46±0.07 (-37.6%)</b>
PushCube	0.13±0.05 (-56.0%)	0.05±0.03 (-89.5%)	0.12±0.09 (-74.3%)	0.31±0.03 (-33.4%)	<b>0.63±0.12 (-39.3%)</b>
PlaceAppleInBowl	0.02±0.02 (-66.4%)	0.03±0.02 (-81.0%)	0.03±0.02 (-79.0%)	0.09±0.04 (-21.7%)	<b>0.28±0.15 (-11.1%)</b>
TransportBox	0.03±0.04 (-37.4%)	0.04±0.04 (-84.6%)	0.19±0.08 (-27.4%)	0.21±0.09 (-15.7%)	<b>0.28±0.01 (-0.7%)</b>

Table 26: Medium Table Texture Test

Task	SAC AE	DrQ-v2	MaDi	SADA	SegDAC
LiftPegUpright	0.21±0.01 (-2.5%)	0.19±0.00 (-60.2%)	0.22±0.01 (-1.1%)	0.22±0.04 (-2.3%)	<b>0.41±0.15 (-1.3%)</b>
PickCube	0.11±0.04 (-39.8%)	0.02±0.01 (-96.4%)	<b>0.30±0.08 (-30.9%)</b>	0.15±0.05 (-61.2%)	0.23±0.06 (-32.8%)
PokeCube	0.12±0.02 (-25.6%)	0.03±0.02 (-92.2%)	<b>0.37±0.07 (-8.7%)</b>	0.17±0.03 (-55.3%)	0.32±0.04 (-18.8%)
PullCube	0.06±0.03 (-82.4%)	0.01±0.00 (-97.0%)	0.41±0.07 (-17.0%)	0.37±0.08 (-23.4%)	<b>0.49±0.04 (-2.3%)</b>
PullCubeTool	0.06±0.09 (-72.1%)	0.05±0.09 (-92.3%)	0.54±0.19 (-13.4%)	0.09±0.10 (-75.0%)	<b>0.64±0.13 (-13.3%)</b>
PushCube	0.19±0.04 (-36.0%)	0.02±0.02 (-95.3%)	0.40±0.08 (-13.0%)	0.21±0.06 (-54.5%)	<b>0.43±0.07 (-3.6%)</b>
PlaceAppleInBowl	0.01±0.00 (-90.7%)	0.02±0.01 (-90.5%)	0.01±0.02 (-88.8%)	0.04±0.02 (-64.5%)	<b>0.29±0.14 (-8.6%)</b>
TransportBox	0.05±0.03 (+2.9%)	0.14±0.04 (-45.6%)	0.23±0.03 (-13.0%)	0.17±0.10 (-28.8%)	<b>0.28±0.01 (+0.2%)</b>

Table 27: Hard Camera Fov Test

Task	SAC AE	DrQ-v2	MaDi	SADA	SegDAC
LiftPegUpright	0.19±0.00 (-12.7%)	0.19±0.01 (-59.9%)	<b>0.20±0.01 (-10.2%)</b>	<b>0.20±0.02 (-9.5%)</b>	<b>0.20±0.01 (-51.8%)</b>
PickCube	0.02±0.01 (-91.6%)	0.02±0.00 (-95.0%)	0.03±0.03 (-93.0%)	0.06±0.03 (-84.0%)	<b>0.07±0.02 (-78.7%)</b>
PokeCube	0.02±0.02 (-89.9%)	0.02±0.01 (-95.2%)	0.02±0.02 (-94.2%)	<b>0.06±0.03 (-85.1%)</b>	0.05±0.01 (-86.3%)
PullCube	0.06±0.03 (-83.6%)	0.01±0.00 (-96.4%)	0.05±0.02 (-89.7%)	0.09±0.03 (-81.2%)	<b>0.11±0.01 (-77.1%)</b>
PullCubeTool	0.02±0.03 (-92.8%)	0.02±0.03 (-96.3%)	0.05±0.02 (-92.2%)	0.03±0.03 (-91.9%)	<b>0.16±0.04 (-78.6%)</b>
PushCube	0.01±0.01 (-95.6%)	0.02±0.03 (-95.4%)	0.04±0.02 (-91.4%)	0.07±0.02 (-85.2%)	<b>0.12±0.05 (-72.5%)</b>
PlaceAppleInBowl	0.01±0.00 (-90.2%)	0.01±0.01 (-91.0%)	0.02±0.02 (-85.7%)	0.02±0.01 (-81.8%)	<b>0.03±0.01 (-90.8%)</b>
TransportBox	0.03±0.03 (-46.0%)	0.10±0.03 (-62.7%)	0.04±0.01 (-84.6%)	0.11±0.04 (-54.0%)	<b>0.28±0.01 (-0.6%)</b>

Table 28: Hard Camera Pose Test

Task	SAC AE	DrQ-v2	MaDi	SADA	SegDAC
LiftPegUpright	0.19±0.00 (-11.6%)	0.19±0.00 (-59.7%)	0.19±0.00 (-13.4%)	<b>0.20±0.01 (-10.0%)</b>	<b>0.20±0.01 (-52.1%)</b>
PickCube	0.01±0.01 (-92.1%)	0.02±0.01 (-96.7%)	0.03±0.02 (-94.2%)	0.03±0.01 (-93.1%)	<b>0.07±0.01 (-79.4%)</b>
PokeCube	0.01±0.01 (-92.1%)	0.01±0.01 (-97.2%)	0.03±0.02 (-93.1%)	<b>0.06±0.02 (-84.9%)</b>	0.05±0.00 (-87.2%)
PullCube	0.02±0.01 (-94.5%)	0.01±0.01 (-98.3%)	0.02±0.01 (-95.3%)	<b>0.05±0.02 (-88.9%)</b>	<b>0.05±0.04 (-89.1%)</b>
PullCubeTool	0.02±0.03 (-92.3%)	0.01±0.01 (-98.1%)	0.01±0.01 (-97.6%)	0.03±0.02 (-90.9%)	<b>0.09±0.05 (-87.3%)</b>
PushCube	0.04±0.03 (-86.7%)	0.01±0.01 (-97.1%)	0.02±0.02 (-95.2%)	0.02±0.01 (-96.6%)	<b>0.10±0.06 (-78.3%)</b>
PlaceAppleInBowl	0.01±0.00 (-93.1%)	0.01±0.01 (-94.5%)	0.01±0.02 (-90.1%)	<b>0.03±0.04 (-71.0%)</b>	<b>0.03±0.02 (-90.9%)</b>
TransportBox	0.03±0.03 (-42.1%)	0.02±0.03 (-91.0%)	0.03±0.03 (-90.4%)	0.06±0.03 (-74.1%)	<b>0.28±0.01 (-1.1%)</b>

Table 29: Hard Ground Color Test

Task	SAC AE	DrQ-v2	MaDi	SADA	SegDAC
LiftPegUpright	0.20±0.01 (-4.6%)	0.19±0.01 (-59.7%)	0.22±0.01 (+0.4%)	0.21±0.01 (-6.5%)	<b>0.38±0.14 (-8.5%)</b>
PickCube	0.02±0.01 (-89.6%)	0.01±0.01 (-96.8%)	<b>0.38±0.06 (-14.2%)</b>	0.09±0.07 (-75.6%)	0.36±0.03 (+6.0%)
PokeCube	0.08±0.02 (-50.3%)	0.01±0.01 (-97.0%)	0.34±0.12 (-16.7%)	0.10±0.03 (-74.2%)	<b>0.35±0.04 (-10.3%)</b>
PullCube	0.01±0.01 (-96.2%)	0.02±0.03 (-94.1%)	0.23±0.21 (-52.3%)	0.38±0.08 (-21.2%)	<b>0.52±0.08 (+3.2%)</b>
PullCubeTool	0.07±0.04 (-66.3%)	0.06±0.06 (-90.4%)	0.46±0.17 (-25.5%)	0.06±0.06 (-84.0%)	<b>0.60±0.14 (-18.5%)</b>
PushCube	0.08±0.05 (-74.7%)	0.02±0.01 (-96.7%)	0.29±0.13 (-38.4%)	0.34±0.10 (-26.3%)	<b>0.47±0.04 (+5.2%)</b>
PlaceAppleInBowl	0.00±0.00 (-96.1%)	0.00±0.00 (-97.4%)	0.03±0.06 (-76.1%)	0.06±0.03 (-50.9%)	<b>0.30±0.16 (-4.0%)</b>
TransportBox	0.05±0.05 (+4.5%)	0.01±0.02 (-95.3%)	0.26±0.02 (-0.6%)	0.23±0.10 (-8.0%)	<b>0.28±0.01 (-0.4%)</b>

Table 30: Hard Ground Texture Test

Task	SAC AE	DrQ-v2	MaDi	SADA	SegDAC
LiftPegUpright	0.21±0.01 (-0.9%)	0.20±0.01 (-57.0%)	0.22±0.01 (+0.0%)	0.21±0.02 (-4.6%)	<b>0.40±0.15 (-2.1%)</b>
PickCube	0.07±0.02 (-61.4%)	0.10±0.06 (-78.9%)	<b>0.43±0.07 (-3.0%)</b>	0.36±0.05 (-6.8%)	0.32±0.02 (-4.2%)
PokeCube	0.10±0.03 (-40.4%)	0.14±0.10 (-67.0%)	<b>0.40±0.01 (-2.1%)</b>	0.27±0.09 (-30.8%)	0.38±0.04 (-3.3%)
PullCube	0.13±0.04 (-64.5%)	0.14±0.06 (-61.1%)	0.31±0.09 (-37.8%)	0.42±0.16 (-14.8%)	<b>0.55±0.05 (+9.6%)</b>
PullCubeTool	0.09±0.04 (-56.6%)	0.08±0.19 (-86.8%)	0.55±0.19 (-12.1%)	0.23±0.07 (-37.2%)	<b>0.68±0.12 (-8.7%)</b>
PushCube	0.12±0.04 (-59.1%)	0.25±0.21 (-46.1%)	0.47±0.09 (+1.9%)	0.39±0.07 (-15.6%)	<b>0.49±0.07 (+9.4%)</b>
PlaceAppleInBowl	0.01±0.00 (-89.1%)	0.00±0.01 (-97.1%)	0.01±0.02 (-88.9%)	0.01±0.01 (-89.3%)	<b>0.27±0.14 (-14.7%)</b>
TransportBox	0.04±0.03 (-12.7%)	0.10±0.11 (-62.2%)	0.07±0.06 (-71.6%)	0.08±0.05 (-66.1%)	<b>0.27±0.01 (-1.6%)</b>

Table 31: Hard Lighting Color Test

Task	SAC AE	DrQ-v2	MaDi	SADA	SegDAC
LiftPegUpright	0.22±0.01 (+0.6%)	0.20±0.01 (-58.6%)	0.20±0.01 (-8.9%)	0.22±0.04 (-2.2%)	<b>0.39±0.15 (-4.4%)</b>
PickCube	0.02±0.01 (-91.2%)	0.01±0.02 (-98.0%)	0.07±0.03 (-83.7%)	0.07±0.02 (-82.5%)	<b>0.15±0.01 (-55.8%)</b>
PokeCube	0.08±0.02 (-53.6%)	0.03±0.01 (-93.2%)	0.21±0.04 (-49.2%)	0.19±0.03 (-51.5%)	<b>0.37±0.05 (-4.8%)</b>
PullCube	0.02±0.01 (-93.4%)	0.04±0.04 (-89.0%)	0.42±0.08 (-14.3%)	0.23±0.10 (-53.7%)	<b>0.49±0.09 (-2.1%)</b>
PullCubeTool	0.01±0.02 (-94.2%)	0.03±0.02 (-95.6%)	0.08±0.05 (-87.5%)	0.17±0.12 (-52.3%)	<b>0.57±0.15 (-23.3%)</b>
PushCube	0.06±0.01 (-78.4%)	0.04±0.02 (-90.4%)	0.36±0.09 (-21.6%)	0.35±0.09 (-23.1%)	<b>0.54±0.05 (+21.0%)</b>
PlaceAppleInBowl	0.01±0.01 (-89.8%)	0.01±0.00 (-95.2%)	0.01±0.02 (-93.0%)	0.07±0.02 (-43.4%)	<b>0.25±0.12 (-21.2%)</b>
TransportBox	0.05±0.03 (+2.2%)	0.26±0.07 (-0.3%)	0.26±0.01 (+0.1%)	0.25±0.09 (+0.0%)	<b>0.28±0.01 (-0.2%)</b>

Table 32: Hard Lighting Direction Test

Task	SAC AE	DrQ-v2	MaDi	SADA	SegDAC
LiftPegUpright	0.21±0.01 (-1.9%)	0.19±0.01 (-59.5%)	0.22±0.01 (+2.3%)	0.22±0.05 (-0.3%)	<b>0.37±0.12 (-10.3%)</b>
PickCube	0.10±0.02 (-44.6%)	0.02±0.01 (-94.6%)	<b>0.40±0.08 (-8.9%)</b>	0.35±0.04 (-10.8%)	0.19±0.02 (-43.1%)
PokeCube	0.13±0.01 (-22.5%)	0.07±0.04 (-84.9%)	<b>0.40±0.02 (-2.2%)</b>	0.35±0.07 (-10.0%)	0.20±0.05 (-49.3%)
PullCube	0.17±0.04 (-54.5%)	0.05±0.07 (-87.7%)	0.45±0.04 (-8.7%)	<b>0.52±0.19 (+7.1%)</b>	0.47±0.08 (-5.8%)
PullCubeTool	0.17±0.04 (-24.2%)	0.04±0.18 (-92.9%)	0.61±0.18 (-1.4%)	0.32±0.09 (-11.5%)	<b>0.64±0.09 (-13.7%)</b>
PushCube	0.21±0.02 (-29.7%)	0.05±0.04 (-89.4%)	0.43±0.07 (-6.9%)	<b>0.44±0.03 (-4.3%)</b>	<b>0.44±0.05 (-2.7%)</b>
PlaceAppleInBowl	0.07±0.02 (-3.1%)	0.01±0.01 (-91.3%)	0.11±0.04 (-9.0%)	0.10±0.04 (-15.9%)	<b>0.24±0.11 (-25.5%)</b>
TransportBox	0.05±0.03 (+1.3%)	0.26±0.07 (-0.7%)	0.26±0.01 (+0.0%)	0.24±0.09 (-0.5%)	<b>0.28±0.01 (+0.5%)</b>

Table 33: Hard Mo Color Test

Task	SAC AE	DrQ-v2	MaDi	SADA	SegDAC
LiftPegUpright	0.21±0.01 (-1.6%)	0.19±0.00 (-59.4%)	0.20±0.00 (-8.9%)	0.20±0.01 (-10.3%)	<b>0.39±0.12 (-5.6%)</b>
PickCube	0.06±0.02 (-68.2%)	0.02±0.01 (-96.6%)	0.01±0.01 (-98.1%)	0.04±0.02 (-90.0%)	<b>0.28±0.03 (-17.2%)</b>
PokeCube	0.08±0.01 (-53.1%)	0.01±0.01 (-97.1%)	0.01±0.00 (-97.2%)	0.02±0.03 (-96.0%)	<b>0.34±0.05 (-13.8%)</b>
PullCube	0.10±0.04 (-73.3%)	0.08±0.01 (-79.5%)	0.12±0.04 (-75.8%)	0.09±0.04 (-81.1%)	<b>0.48±0.07 (-3.9%)</b>
PullCubeTool	0.04±0.02 (-80.4%)	0.05±0.12 (-91.8%)	0.07±0.04 (-89.0%)	0.19±0.17 (-46.8%)	<b>0.44±0.10 (-40.2%)</b>
PushCube	0.10±0.02 (-65.9%)	0.02±0.00 (-96.4%)	0.08±0.03 (-82.7%)	0.06±0.02 (-88.0%)	<b>0.48±0.05 (+7.0%)</b>
PlaceAppleInBowl	0.02±0.01 (-78.6%)	0.01±0.00 (-92.9%)	0.06±0.02 (-51.9%)	0.06±0.03 (-46.2%)	<b>0.30±0.17 (-6.4%)</b>
TransportBox	0.05±0.03 (+1.8%)	0.18±0.11 (-30.1%)	0.26±0.01 (-0.9%)	0.24±0.10 (-2.2%)	<b>0.28±0.01 (-0.2%)</b>

Table 34: Hard Mo Texture Test

Task	SAC AE	DrQ-v2	MaDi	SADA	SegDAC
LiftPegUpright	0.20±0.01 (-5.1%)	0.22±0.01 (-53.9%)	0.21±0.01 (-4.4%)	0.22±0.02 (-1.2%)	<b>0.28±0.08 (-32.3%)</b>
PickCube	0.06±0.02 (-69.8%)	0.01±0.00 (-97.0%)	0.01±0.00 (-98.1%)	0.02±0.01 (-94.4%)	<b>0.15±0.01 (-55.2%)</b>
PokeCube	0.08±0.01 (-54.2%)	0.03±0.01 (-92.1%)	0.04±0.09 (-89.4%)	0.02±0.02 (-95.1%)	<b>0.22±0.03 (-45.0%)</b>
PullCube	0.12±0.04 (-66.5%)	0.10±0.03 (-71.4%)	0.26±0.12 (-46.2%)	0.10±0.04 (-79.0%)	<b>0.43±0.05 (-14.4%)</b>
PullCubeTool	0.13±0.04 (-40.8%)	0.12±0.08 (-81.2%)	0.03±0.02 (-94.6%)	0.02±0.05 (-94.0%)	<b>0.45±0.08 (-38.9%)</b>
PushCube	0.13±0.02 (-55.9%)	0.02±0.02 (-94.9%)	0.15±0.07 (-67.7%)	0.08±0.03 (-82.7%)	<b>0.45±0.06 (-0.4%)</b>
PlaceAppleInBowl	0.05±0.02 (-32.0%)	0.05±0.03 (-70.3%)	0.06±0.02 (-54.9%)	0.04±0.04 (-66.6%)	<b>0.29±0.18 (-7.4%)</b>
TransportBox	0.05±0.03 (+1.6%)	0.18±0.07 (-28.9%)	0.26±0.01 (-0.1%)	0.23±0.09 (-5.2%)	<b>0.28±0.01 (-0.1%)</b>

Table 35: Hard Ro Color Test

Task	SAC AE	DrQ-v2	MaDi	SADA	SegDAC
LiftPegUpright	N/A	N/A	N/A	N/A	N/A
PickCube	N/A	N/A	N/A	N/A	N/A
PokeCube	0.11±0.03 (-34.2%)	0.06±0.01 (-85.9%)	0.30±0.07 (-27.9%)	0.20±0.06 (-49.0%)	<b>0.39±0.05 (+0.0%)</b>
PullCube	0.04±0.02 (-88.0%)	0.01±0.01 (-96.4%)	0.09±0.12 (-82.1%)	0.09±0.08 (-81.3%)	<b>0.50±0.05 (-1.2%)</b>
PullCubeTool	0.14±0.05 (-35.2%)	0.28±0.09 (-54.7%)	0.42±0.16 (-32.3%)	0.23±0.14 (-38.2%)	<b>0.67±0.18 (-9.0%)</b>
PushCube	0.06±0.01 (-78.9%)	0.04±0.01 (-91.3%)	0.29±0.13 (-38.2%)	0.04±0.02 (-90.7%)	<b>0.46±0.04 (+1.7%)</b>
PlaceAppleInBowl	0.04±0.02 (-52.6%)	0.01±0.01 (-92.4%)	0.07±0.03 (-44.3%)	0.11±0.04 (-11.0%)	<b>0.27±0.12 (-15.6%)</b>
TransportBox	N/A	N/A	N/A	N/A	N/A

Table 36: Hard Ro Texture Test

Task	SAC AE	DrQ-v2	MaDi	SADA	SegDAC
LiftPegUpright	N/A	N/A	N/A	N/A	N/A
PickCube	N/A	N/A	N/A	N/A	N/A
PokeCube	0.16±0.02 (-4.3%)	0.25±0.01 (-43.2%)	<b>0.40±0.01 (-3.3%)</b>	0.36±0.08 (-6.8%)	0.30±0.06 (-23.7%)
PullCube	0.29±0.08 (-20.7%)	0.06±0.07 (-84.8%)	0.46±0.12 (-6.3%)	<b>0.54±0.12 (+11.5%)</b>	0.52±0.11 (+3.5%)
PullCubeTool	0.18±0.08 (-17.0%)	0.39±0.18 (-37.5%)	0.61±0.19 (-1.2%)	0.31±0.19 (-16.1%)	<b>0.66±0.16 (-11.1%)</b>
PushCube	0.27±0.05 (-10.7%)	0.11±0.11 (-75.4%)	<b>0.51±0.14 (+9.1%)</b>	0.48±0.10 (+4.3%)	0.44±0.07 (-1.5%)
PlaceAppleInBowl	0.08±0.02 (+2.9%)	0.12±0.05 (-24.3%)	0.10±0.06 (-17.0%)	0.13±0.04 (+5.7%)	<b>0.26±0.10 (-16.9%)</b>
TransportBox	N/A	N/A	N/A	N/A	N/A

Table 37: Hard Table Color Test

Task	SAC AE	DrQ-v2	MaDi	SADA	SegDAC
LiftPegUpright	0.19±0.00 (-11.7%)	0.19±0.01 (-60.0%)	0.19±0.00 (-13.0%)	0.22±0.01 (-0.5%)	<b>0.38±0.14 (-8.1%)</b>
PickCube	0.02±0.01 (-88.5%)	0.00±0.00 (-98.9%)	0.02±0.01 (-95.2%)	0.03±0.01 (-92.2%)	<b>0.11±0.01 (-67.9%)</b>
PokeCube	0.02±0.01 (-90.5%)	0.02±0.01 (-95.7%)	0.03±0.03 (-92.6%)	0.12±0.04 (-68.9%)	<b>0.20±0.03 (-49.9%)</b>
PullCube	0.02±0.02 (-94.0%)	0.02±0.02 (-95.9%)	0.09±0.04 (-81.0%)	0.27±0.04 (-43.9%)	<b>0.35±0.07 (-31.1%)</b>
PullCubeTool	0.03±0.02 (-85.9%)	0.03±0.02 (-95.9%)	0.03±0.03 (-94.9%)	0.02±0.03 (-95.5%)	<b>0.14±0.04 (-80.9%)</b>
PushCube	0.04±0.03 (-87.0%)	0.04±0.03 (-91.0%)	0.06±0.03 (-86.3%)	0.17±0.08 (-64.1%)	<b>0.60±0.15 (+33.3%)</b>
PlaceAppleInBowl	0.00±0.01 (-93.4%)	0.01±0.01 (-92.7%)	0.01±0.02 (-95.5%)	0.04±0.05 (-67.5%)	<b>0.25±0.09 (-21.2%)</b>
TransportBox	0.07±0.05 (+45.2%)	0.07±0.10 (-73.6%)	0.12±0.06 (-55.8%)	0.19±0.10 (-20.7%)	<b>0.28±0.01 (-0.6%)</b>

Table 38: Hard Table Texture Test

Task	SAC AE	DrQ-v2	MaDi	SADA	SegDAC
LiftPegUpright	0.19±0.01 (-10.9%)	<b>0.20±0.01 (-58.3%)</b>	<b>0.20±0.01 (-11.2%)</b>	<b>0.20±0.01 (-8.7%)</b>	<b>0.20±0.01 (-51.7%)</b>
PickCube	0.03±0.01 (-83.7%)	0.02±0.01 (-96.0%)	0.05±0.04 (-89.4%)	<b>0.07±0.03 (-82.5%)</b>	<b>0.07±0.02 (-79.9%)</b>
PokeCube	0.07±0.05 (-54.9%)	0.02±0.00 (-96.0%)	0.06±0.03 (-85.4%)	0.08±0.02 (-78.2%)	<b>0.15±0.04 (-62.3%)</b>
PullCube	0.03±0.02 (-93.0%)	0.01±0.00 (-98.4%)	0.12±0.04 (-75.2%)	<b>0.16±0.04 (-67.7%)</b>	0.04±0.03 (-92.5%)
PullCubeTool	0.07±0.07 (-67.7%)	0.03±0.03 (-94.6%)	<b>0.29±0.17 (-53.0%)</b>	0.05±0.03 (-86.5%)	0.02±0.02 (-97.4%)
PushCube	0.04±0.01 (-86.2%)	0.03±0.02 (-92.4%)	0.05±0.03 (-90.2%)	0.08±0.02 (-83.7%)	<b>0.10±0.06 (-78.2%)</b>
PlaceAppleInBowl	0.01±0.00 (-82.9%)	0.01±0.02 (-91.9%)	0.01±0.02 (-91.3%)	0.05±0.02 (-56.9%)	<b>0.25±0.11 (-20.2%)</b>
TransportBox	0.05±0.04 (+7.6%)	0.15±0.08 (-41.3%)	0.24±0.04 (-9.3%)	0.25±0.08 (+3.7%)	<b>0.27±0.01 (-2.2%)</b>

## B Ablations

### B.1 Text Prompts Ablation

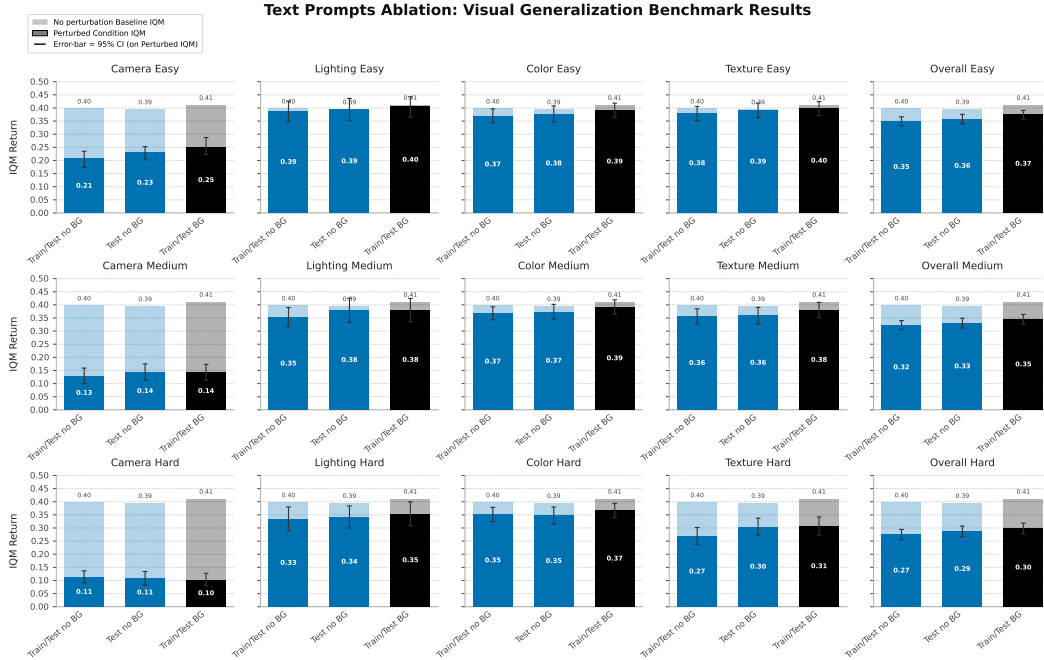


Figure 24: Visual generalization results for the different text tags ablations.

We conducted an ablation to evaluate whether including the "background" text tag improves visual generalization in SegDAC. In the "Train/Test no BG" setting (Figure 24), the model is trained and tested without the "background" tag. For example, in the Push Cube task, the input tags would be ["robot", "gripper", "small box", "target"] instead of ["background", "robot", "gripper", "small box", "target"]. In the "Test no BG" setting, the model is trained with the background tag but tested without it. The final configuration, shown in black in Figure 24, uses the background tag during both training and testing and corresponds to the final version of SegDAC.

The goal of this ablation is to determine whether training with background segments encourages the model to ignore irrelevant information more effectively, or if excluding them allows it to focus more directly on task-relevant objects. While YOLO-World and SAM can still introduce irrelevant segments even without the background tag, our experiments show that including the tag leads to a noticeably larger number of irrelevant segments.

Results in Figure 24 show that all configurations perform similarly, but "Train/Test BG" achieves about  $\sim 9\%$  higher IQM returns. This suggests that including the background tag improves generalization by encouraging the model to focus less on distractions.

### B.2 Object-Centric vs Global Image Representations

To assess whether object-centric representations are more effective than global image features, we compared SegDAC to an SAC baseline that uses a fixed-length global image representation. This baseline, referred to as SAC SAM Encoder, computes the mean of SAM's patch embeddings over the entire image, without using segmentation. The resulting vector is then processed by an MLP with the same number of layers as the projection head used in SegDAC to predict actions or Q-values.

Figure 25 shows the results. SegDAC outperforms SAC SAM Encoder on 7 out of 8 tasks and ties on the remaining one. This highlights a key limitation of directly using pre-trained encoders like SAM for global image representations in online visual RL. Even after attempting hyperparameter tuning for SAC SAM Encoder, we observed no improvement in performance.

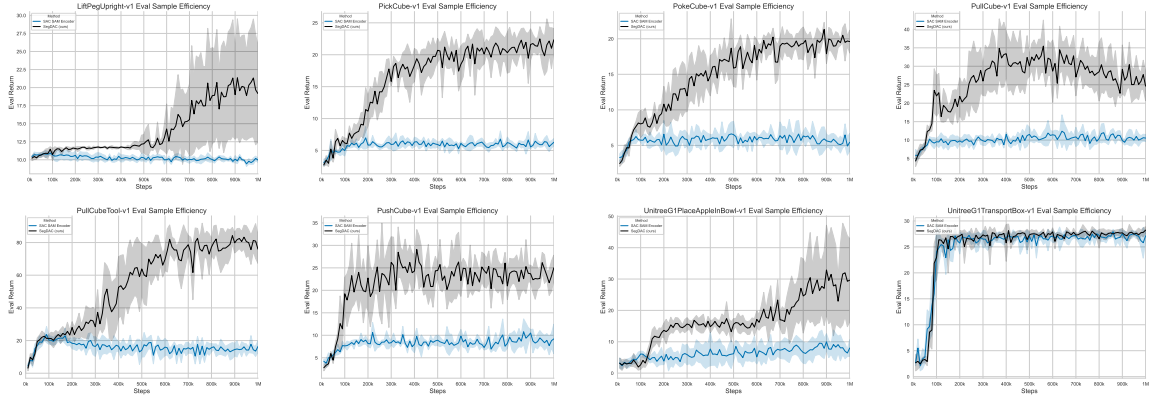


Figure 25: Sample efficiency comparison of SegDAC vs SAC SAM Encoder which uses a global image representation instead of the object-centric representations used by SegDAC.

## C Tasks Definitions

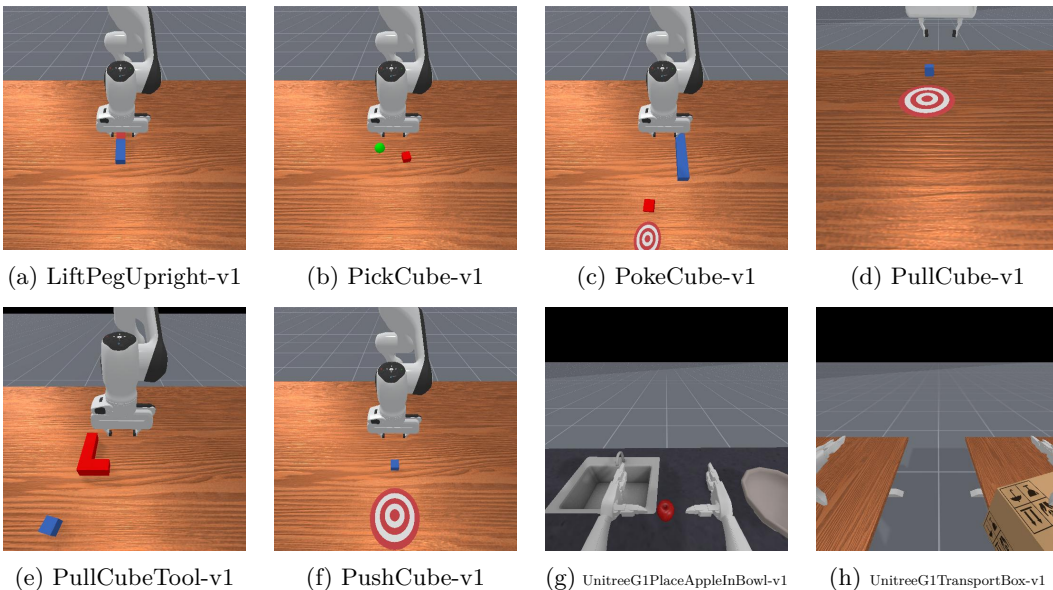


Figure 26: Default (no perturbation) scenes for each of the 8 tasks used for training.

To train SegDAC and the baselines, we used 8 tasks from ManiSkill3 (version `mani_skill==3.0.0b21`) with the default normalized dense reward. The tasks and their corresponding configurations are summarized in table 39 and visualized in figure 26.

Task Name	Max Episode Length	Control Mode
LiftPegUpright-v1	50	PD EE Delta Pos
PickCube-v1*	50	PD EE Delta Pos
PokeCube-v1	50	PD EE Delta Pos
PullCube-v1	50	PD EE Delta Pos
PullCubeTool-v1	100	PD EE Delta Pos
PushCube-v1	50	PD EE Delta Pos
UnitreeG1PlaceAppleInBowl-v1	100	PD Joint Delta Pos
UnitreeG1TransportBox-v1	100	PD Joint Delta Pos

Table 39: Task configurations used for training SegDAC and baselines.

\* For the PickCube-v1 task, we created a modified version that makes the visual target sphere visible. This allows vision-based policies to leverage goal information. We achieved this by commenting out the following line in the original task code:

```
# self._hidden_objects.append(self.goal_site)
```

## D Hyperparameters

Each method was trained using its own hyperparameter configuration. Once a configuration was found to perform well for a given method, it was kept fixed across all tasks. For the baselines, we used the official implementations provided by the authors and used their default hyperparameters as starting points. In most cases, these settings were appropriate without modification. The only adjustment we made was to the discount factor, which we set to 0.80 for all methods, as we found this value worked better with ManiSkill3 and is also used in the framework’s official baselines.

For SegDAC, text tags were provided manually per task by a human. However, automatic tagging is also feasible using a VLM or image text tagging models such as RAM++ [Zhang et al. \(2023a\)](#). We opted for manual tags to reduce the scope of this research and to reduce computational overhead. We did not perform extensive tuning of the tags, instead, we selected simple text tags that seemed to make sense given a static frame and verified that SAM produced reasonable segmentations for them. While more exploration is needed to determine the optimal tags, we found that basic tags performed well in practice.

Note that due to computational constraints, we did not perform an extensive hyperparameter search for SegDAC, and we did not tune the parameters of YOLO-World or SAM.

Tables 41 and 42 summarize the key hyperparameters used for SegDAC and the baselines. We report only the most relevant parameters for reproducibility, omitting architectural defaults that are standard for each algorithm. For the complete list of hyperparameters, readers are invited to check the official code repository on the project page <https://segdac.github.io/>

Table 40: Text tags used by SegDAC for each task.

Task	Text Tags
LiftPegUpright-v1	background, robot, gripper, rectangle bar, wooden peg
PickCube-v1	background, robot, gripper, small box, sphere
PushCube-v1	background, robot, gripper, small box, target
PullCube-v1	background, robot, gripper, small box, target
PokeCube-v1	background, robot, gripper, small box, bar, target
PullCubeTool-v1	background, robot, gripper, small box, block
UnitreeG1PlaceAppleInBowl-v1	background, robot, robot hand, gripper, apple, bowl
UnitreeG1TransportBox-v1	background, robot, robot hand, gripper, box

The list of text tags used by SegDAC for each task is provided in Table 40.

Hyperparameter	SegDAC
Actor learning rate	$3 \times 10^{-4}$
Critic learning rate	$5 \times 10^{-4}$
Entropy learning rate	$3 \times 10^{-4}$
Optimizer	Adam
Gamma (discount)	0.80
Target update rate ( $\tau$ )	0.01
Actor update frequency	1
Critic update frequency	1
Target networks update frequency	2
Image resolution	512
Min log std	-10
Max log std	2
Embedding dim	128
Transformer decoder layers	6
Transformer decoder heads	8
Transformer decoder hidden size	1024
Transformer dropout	0.0
Projection head	ResidualMLP
Projection head hidden layers	4
Projection head hidden size	256
Projection head norm	LayerNorm
Projection head pre-normalize input	true
Projection head activation	ReLU
YOLO-World	yolov8s-worldv2
YOLO-World Confidence Threshold	0.0001
YOLO-World IoU Threshold	0.01
EfficientViT SAM	efficientvit-sam-l0
Mask post-processing kernel size	9
Segment Embedding Min Pixel	4
Replay Buffer Max Size	1,000,000

Table 41: Key hyperparameters used for training SegDAC.

Note that in SegDAC, the actor and critic each use their own transformer decoder and projection head, but they share the same architecture and hyperparameters. For clarity, we omit separate entries for each and report the shared configuration.

Hyperparameter	SADA	MaDi	DrQ-v2	SAC-AE	SAC State
Actor learning rate	$5 \times 10^{-4}$	$1 \times 10^{-3}$	$1 \times 10^{-4}$	$1 \times 10^{-4}$	$3 \times 10^{-4}$
Critic learning rate	$5 \times 10^{-4}$	$1 \times 10^{-3}$	$1 \times 10^{-4}$	$1 \times 10^{-3}$	$3 \times 10^{-3}$
Entropy learning rate	$5 \times 10^{-4}$	$1 \times 10^{-4}$	-	$1 \times 10^{-4}$	$3 \times 10^{-4}$
Target update rate ( $\tau$ )	0.01	0.01	0.01	0.01	0.01
Actor update frequency	2	2	2	1	1
Critic update frequency	2	1	2	1	1
Target networks update frequency	2	2	2	2	2
Replay buffer size	1,000,000	1,000,000	1,000,000	1,000,000	1,000,000
Gamma (discount)	0.80	0.80	0.80	0.80	0.80
Image resolution	84	84	84	84	-
MLP Projection layers	4	3	4	3	4
MLP Projection dim	1024	1024	1024	1024	256
Frame Stack	3	3	3	3	3
N-step return	-	-	3	-	-
Optimizer	Adam	Adam	Adam	Adam	Adam

Table 42: Key hyperparameters for baseline methods. SAC State uses privileged full state information instead of images.

## E Segmentation Details

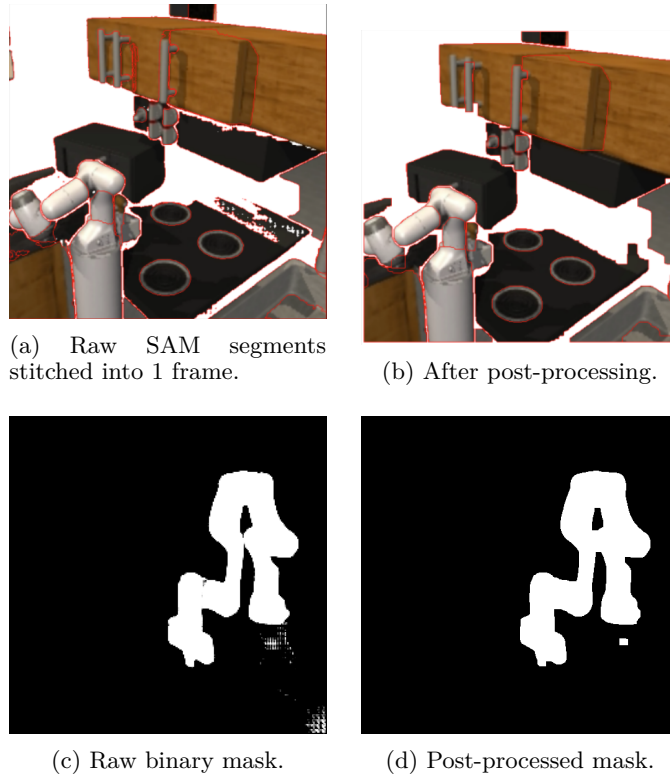


Figure 27: Effect of our lightweight post-processing on SAM outputs. Top: stitched overlays. Bottom: single mask.

To improve the quality of segments predicted by SAM, prior work such as SAM Kirillov et al. (2023), SAM-G Wang et al. (2023), and PerSAM Zhang et al. (2023b) typically rely on heavy post-processing pipelines, often involving iterative mask refinement. In contrast, we adopt a lightweight and efficient approach based on morphological opening and closing operations Sreedhar (2012). These classical image processing techniques are fast and effective at removing small artifacts such as holes or sprinkles commonly found in raw segmentation masks. The impact of this post-processing is illustrated in Figure 27.

Our implementation of this post-processing procedure is written in pure PyTorch, as shown below:

```
import torch
import torch.nn.functional as F

...
def post_process_masks(self, masks: torch.Tensor, kernel_size: int) -> torch.Tensor:
    """
    masks: (N,1,H,W)
    """
    opened = self.apply_morphological_opening(
        masks.to(torch.float32), kernel_size=kernel_size
    )
    return self.apply_morphological_closing(opened, kernel_size=kernel_size).to(
        torch.uint8
```

---

```

    )

def apply_morphological_opening(
    self, masks: torch.Tensor, kernel_size: int
) -> torch.Tensor:
    eroded = self.apply_erosion(masks, kernel_size)
    return self.apply_dilation(eroded, kernel_size)

def apply_erosion(self, masks: torch.Tensor, kernel_size: int) -> torch.Tensor:
    return -self.max_pool2d_same_dim(-masks, kernel_size=kernel_size)

def apply_dilation(self, masks: torch.Tensor, kernel_size: int) -> torch.Tensor:
    return self.max_pool2d_same_dim(masks, kernel_size=kernel_size)

def max_pool2d_same_dim(self, masks: torch.Tensor, kernel_size: int):
    stride = 1
    dilation = 1
    pad_h_top, pad_h_bottom = self.compute_padding(
        kernel_size, stride, dilation)
    pad_w_left, pad_w_right = self.compute_padding(
        kernel_size, stride, dilation)

    padded_input = F.pad(
        masks, (pad_w_left, pad_w_right, pad_h_top, pad_h_bottom))

    return F.max_pool2d(
        padded_input, kernel_size=kernel_size, stride=stride, dilation=dilation
    )

def compute_padding(self, kernel_size, stride=1, dilation=1):
    padding_total = max(0, (kernel_size - 1) * dilation - stride + 1)
    pad_before = padding_total // 2
    pad_after = padding_total - pad_before
    return pad_before, pad_after

def apply_morphological_closing(
    self, masks: torch.Tensor, kernel_size: int
) -> torch.Tensor:
    dilated = self.apply_dilation(masks, kernel_size)
    return self.apply_erosion(dilated, kernel_size)

```

## F Segment Embeddings Extraction Details

Figure 28 illustrates the relationship between the binary masks produced by our grounded segmentation module (left), the corresponding **overlapping** patch embeddings (middle), and a heatmap showing the pixel count per patch (right). Most patch embeddings have a high pixel count, while those near the mask edges tend to overlap less exclusively with the segment.

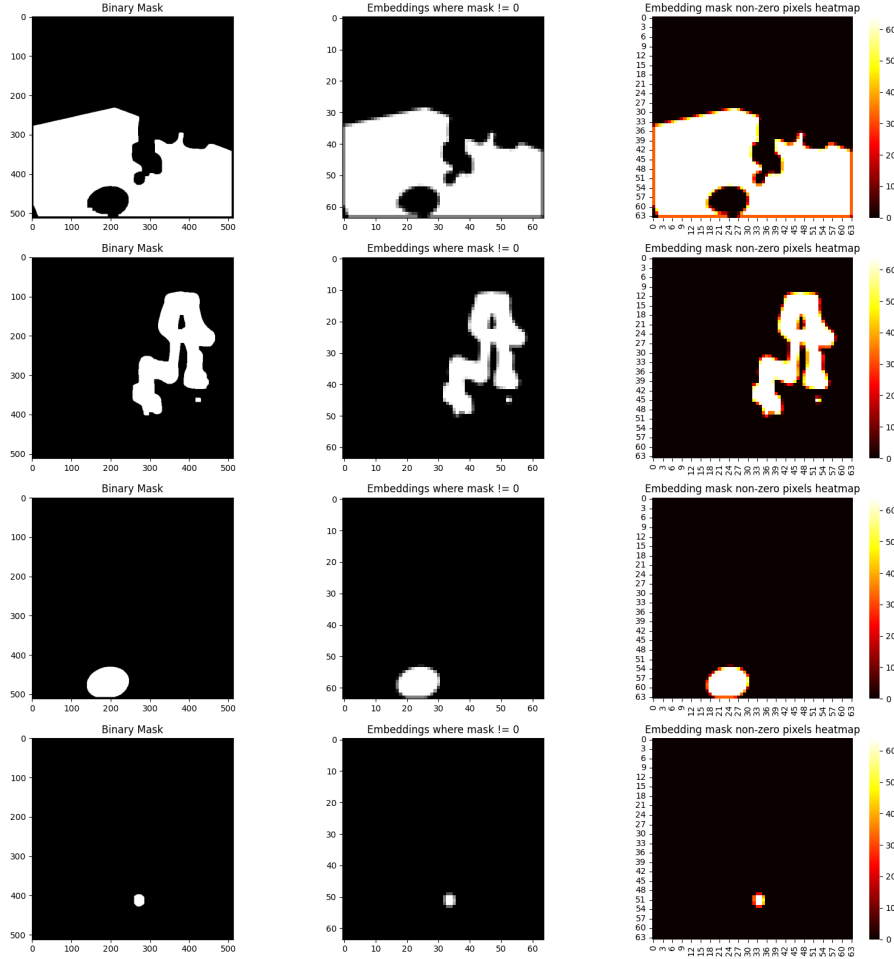


Figure 28: On the left is the binary mask obtained from our grounded segmentation module, in the middle are the patch embeddings from SAM’s encoder when showing only the patch embeddings activated by the mask on the left. On the right is a heatmap showing the number of non-zero pixels in each patch embeddings. A patch embedding can contain information from pixels belonging to multiple segments, especially at the edges, here pixels belonging to other segments are zero-ed out for each segment, this explains the lower number of pixels count at the edges (red color). A patch that is fully white means that all pixels in the patch belong to this segment whereas redder patches have less pixels that only belong to this segment.

## G Robustness to Segment Variability



(a) Few segments detected for an early time step. (b) Significantly more segments detected in a future time step.

Figure 29: Examples of variable segments that can be detected by SAM at different time step for the task UnitreeG1PlaceAppleInBowl-v1.

Figure 29 shows that SegDAC is able to handle a variable number of segments during a rollout even when the number of segments varies significantly, this is a key advantage of SegDAC compared to previous work.

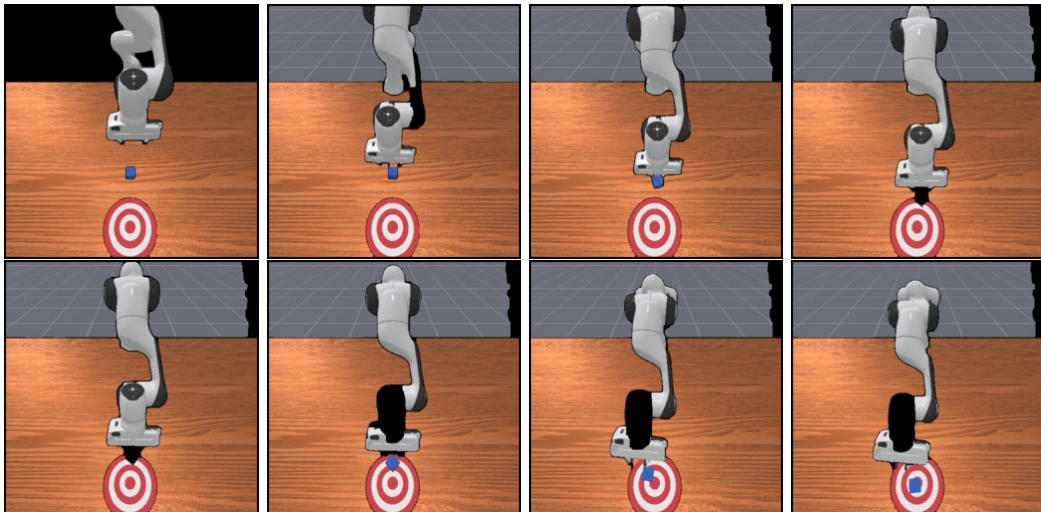


Figure 30: Rollout examples showing segments. For illustration, we stitch all segments into a single frame. Black areas indicate regions where SAM did not detect any segments. The trajectory starts from the top-left frame.

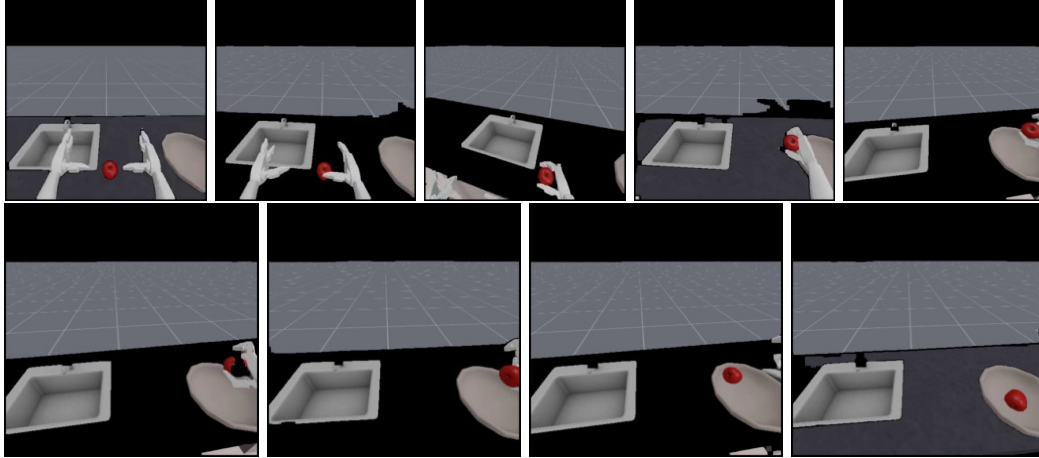


Figure 31: Rollout example showing variability in detected segments, with SegDAC maintaining robust behavior throughout. The trajectory starts from the top-left frame.

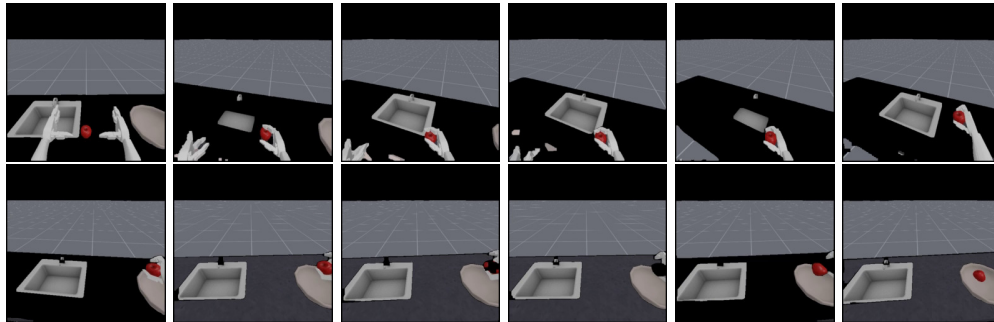


Figure 32: Another rollout example showing variability in detected segments. The trajectory starts from the top-left frame.

Note that while the figures show all segments stitched together into a single frame for visualization purposes, SegDAC still processes them as a sequence of individual segments. Black regions indicate frames where SAM failed to detect certain objects.

Figures 30 to 32 present rollouts in which the set of detected segments varies significantly over time. For example, in Figure 30, the background is initially undetected but later appears, the cube disappears midway through the trajectory, and part of the robot arm is no longer segmented toward the end. Despite such changes, including the temporary disappearance of task-critical segments like the cube or apple, SegDAC maintains robust behavior and handles dynamically changing segment inputs effectively. This robustness is particularly noteworthy given that SegDAC does not rely on temporal smoothing, memory, or frame stacking.

## H Segment Attention Analysis

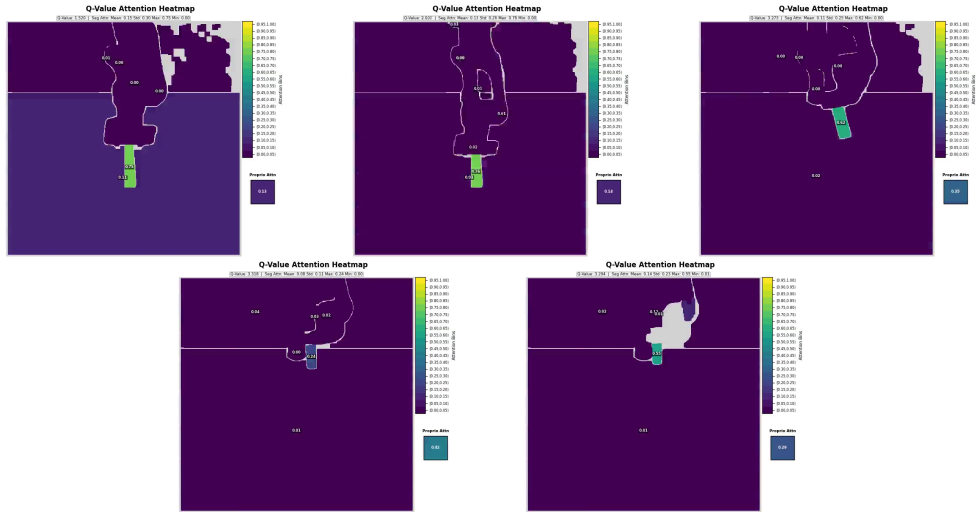


Figure 33: Average segment attention from the critic when predicting Q-values in the LiftPegUpright-v1 task. The trajectory begins in the top-left frame. Grey regions indicate areas where SAM did not detect any segments.

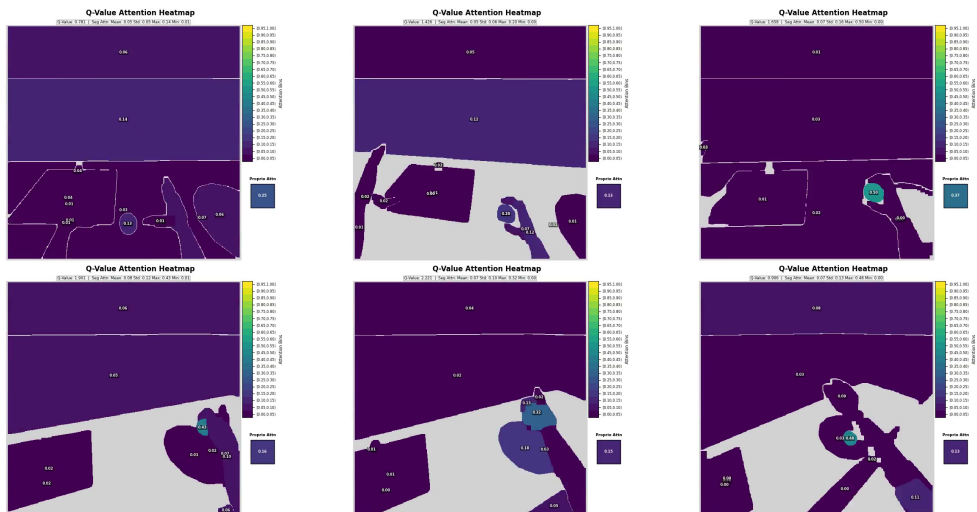


Figure 34: Average segment attention from the critic when predicting Q-values in the UnitreeG1PlaceAppleInBowl-v1 task. The trajectory begins in the top-left frame. Grey regions indicate areas where SAM did not detect any segments.

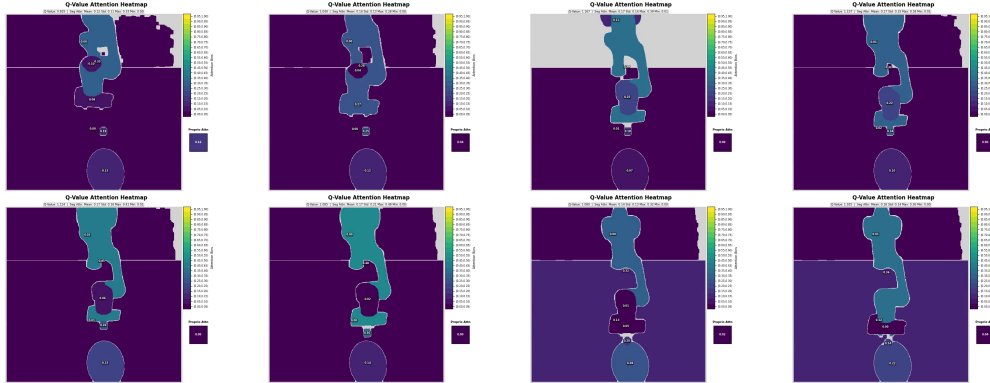


Figure 35: Average segment attention from the critic when predicting Q-values in the PushCube-v1 task. The trajectory begins in the top-left frame. Grey regions indicate areas where SAM did not detect any segments.

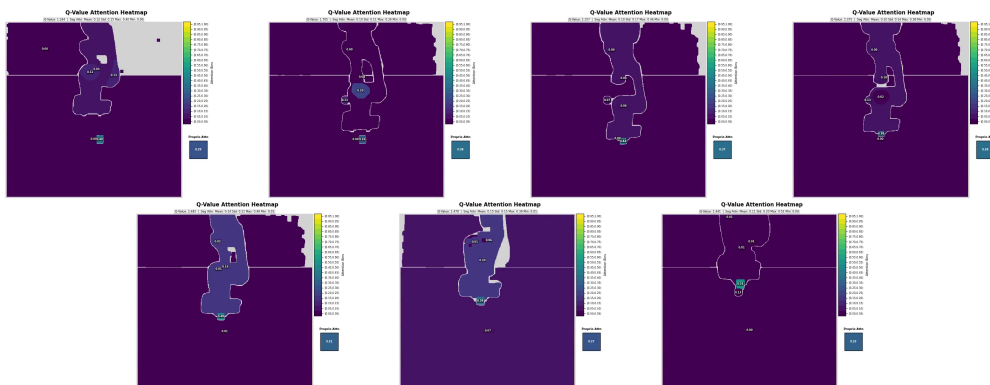


Figure 36: Average segment attention from the critic when predicting Q-values in the PickCube-v1 task. The trajectory begins in the top-left frame. Grey regions indicate areas where SAM did not detect any segments.

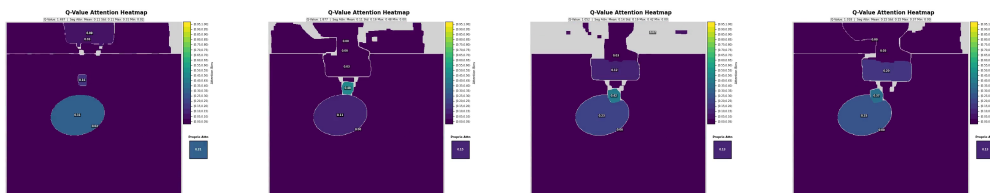


Figure 37: Average segment attention from the critic when predicting Q-values in the PullCube-v1 task. The trajectory begins on the left frame. Grey regions indicate areas where SAM did not detect any segments.

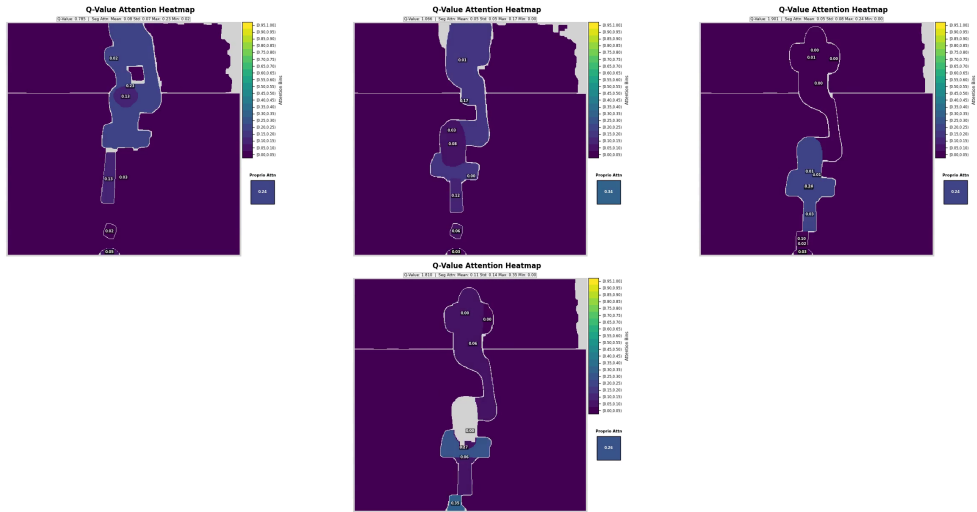


Figure 38: Average segment attention from the critic when predicting Q-values in the PokeCube-v1 task. The trajectory begins in the top-left frame. Grey regions indicate areas where SAM did not detect any segments.

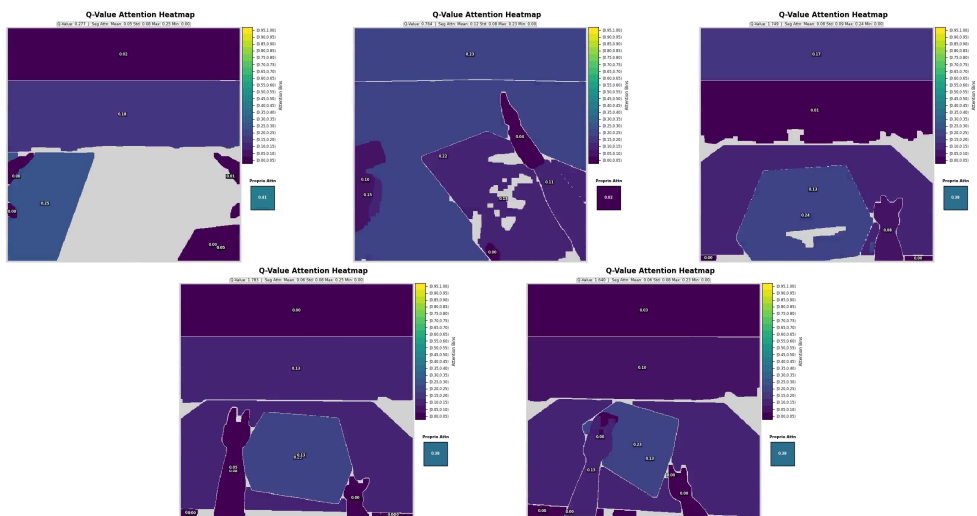


Figure 39: Average segment attention from the critic when predicting Q-values in the UnitreeG1TransportBox-v1 task. The trajectory begins in the top-left frame. Grey regions indicate areas where SAM did not detect any segments.

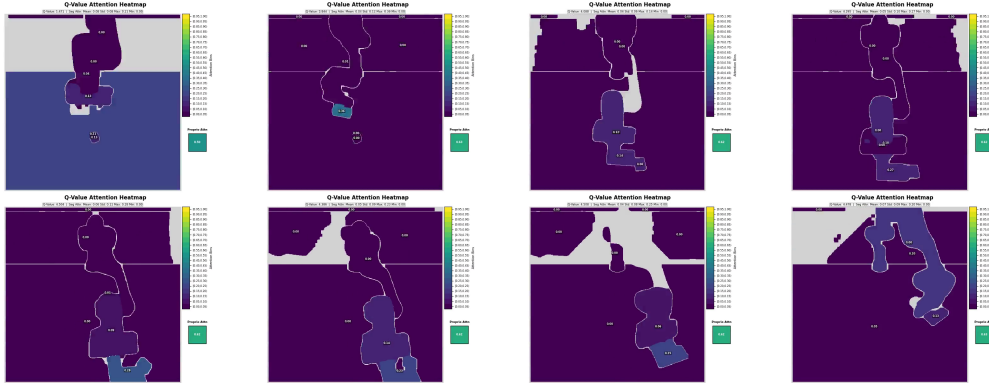


Figure 40: Average segment attention from the critic when predicting Q-values in the PullCubeTool-v1 task. The trajectory begins in the top-left frame. Grey regions indicate areas where SAM did not detect any segments.

Figures 33 to 40 show the average segment attention from the critic when predicting Q-values for all eight tasks. Grey regions indicate areas where SAM did not detect any segments.

We observe that SegDAC consistently attends to task-relevant segments, such as the peg in LiftPegUpright-v1, while ignoring background elements when they provide no useful information. For example, in LiftPegUpright-v1, the peg receives approximately 75% of the attention early in the trajectory. Once the peg is upright, the model shifts some attention to proprioceptive inputs, possibly to stabilize the peg.

SegDAC also demonstrates robustness to variability in detected segments. In PickCube-v1, early frames show the servo button segmented as a small circular region, which the critic uses to guide positioning. In later frames, when the full robot arm is detected instead, the critic adapts and reallocates attention accordingly to complete the task.

Across tasks, SegDAC often allocates significant attention to the manipulation object. For instance, the apple receives about 50% of the attention in UnitreeG1PlaceAppleInBowl-v1. Similarly, in LiftPegUpright-v1, the peg receives around 75% early on.

Figure 36 illustrates that SegDAC is robust to partial occlusions. At the beginning of the trajectory, the goal region is fully occluded by the robot arm, and the model focuses its attention on the cube, which aligns with the sub-goal of grasping it first. As the cube is picked up and the arm moves, the goal region becomes partially visible. Even when it becomes occluded again during the motion, SegDAC continues moving the arm toward the correct location. The goal region becomes visible near the end, and the model successfully completes the task. This shows that SegDAC can handle some level of dynamic occlusions and maintain task-relevant behavior throughout.

Finally, we observe that SegDAC does not maintain uniform attention on the robot throughout the trajectory. In some tasks, the model shifts its focus toward proprioceptive features, while in others it emphasizes the robot arm. We also note that the goal is often ignored initially, especially when the first sub-task is to reach or grasp the manipulation object. Once the object is secured and needs to be moved, the model begins allocating more attention to the goal. This behavior indicates that allowing the model to learn its own attention distribution enables more adaptive and flexible decision-making, as opposed to imposing rigid attention patterns.

---

# I Implementation Details

## I.1 Policy Evaluation and Data Collection

In this work, we use **evaluation** to refer to the policy’s performance under the *no-perturbation* setting during training, which we use to track sample efficiency. In contrast, **testing** refers to performance on the *visual generalization benchmark*, which includes various visual perturbations. This distinction separates standard in-distribution evaluation from robustness testing under distribution shifts.

During both evaluation and testing, stochastic policies were run in deterministic mode by taking the mean of their action distributions. We followed the ManiSkill3 evaluation protocol<sup>1</sup>, which disables early termination to ensure all trajectories have the same length. This makes performance metrics more comparable.

Evaluation metrics were averaged over 5 random seeds, each with 10 rollouts. Proper seeding was applied at the start of both training and evaluation scripts. We used 10 parallel environments to collect evaluation rollouts during training.

For training, we used 20 parallel GPU environments and performed 5 gradient updates per environment step with a batch size of 128, resulting in an update-to-data ratio of 0.25.

## I.2 Online RL Optimization

Training online reinforcement learning agents with large models such as SAM and high resolution images (512×512) can be computationally expensive. To ensure experiments completed within a reasonable time frame (approximately one day on a single L40s GPU), we implemented several optimizations.

**Efficient Vision Backbone.** We replaced the original SAM model Kirillov et al. (2023) with EfficientViT-SAM Zhang et al. (2024), which offers comparable segmentation quality but significantly faster inference speed, approximately 48x faster according to the authors. We also tested SAM 2 Ravi et al. (2024), which improves encoder efficiency but remained significantly slower than EfficientViT-SAM in practice.

All RGB images were processed at a resolution of (3, 512, 512) in (C, H, W) format. This is significantly higher than standard visual RL settings, which often operate in the (3, 84, 84) to (3, 128, 128) range (Laskin et al., 2020; Kostrikov et al., 2021; Srinivas et al., 2020; Hansen and Wang, 2021; Yarats et al., 2021; Bertoin et al., 2023; Almuzairee et al., 2024; Grooten et al., 2023). We used the smallest checkpoint (efficientvit\_sam\_10), which natively supports 512×512 images. Reducing the resolution further led to noticeable performance degradation with only marginal speedup, so we retained the native resolution.

We extended EfficientViT-SAM to support batched image embedding computation. This significantly improved throughput since image embedding is the most computationally expensive step. Most SAM variants, including the official implementations, do not support batching. Additionally, we tested prompt-free segmentation but found it to be too slow for our pipeline (10-100x slower), so we opted for guided segmentation using text prompts.

**Efficient Network Computation.** To optimize network computation, we used `torch.vmap` Paszke et al. (2019) to batch forward passes across multiple networks, such as the twin critics in SAC. This allowed us to compute their outputs in a single pass, improving efficiency.

---

<sup>1</sup>[https://maniskill.readthedocs.io/en/v3.0.0b21/user\\_guide/reinforcement\\_learning/setup.html#evaluation](https://maniskill.readthedocs.io/en/v3.0.0b21/user_guide/reinforcement_learning/setup.html#evaluation)

---

**Replay Buffer Design.** We implemented a custom replay buffer using `TensorDict` [Bou et al. \(2023\)](#) to efficiently handle the variable number of segments per frame. Since the segment embedding extraction module has no trainable weights, we compute embeddings once during data collection and store them directly in the buffer rather than storing raw images.

This approach reduces both memory usage and compute load. Segment embeddings have dimension 128~256, and a typical frame has between 4 and 25 segments, this is significantly smaller than the original ( $3 \times 512 \times 512$ ) image. This also avoids running SAM during training, which would otherwise make online RL infeasible.

**Variable-Length Sequence Handling.** Since each environment step yields a variable number of segments, a batch of  $B$  steps results in a total of  $N_{\text{total}}$  segments. Padding each sequence to a fixed length would be inefficient and would require an additional per-task hyperparameter. To avoid this, we adopt sequence packing, inspired by recent techniques in large language models ([Krell et al., 2022](#)). All segment embeddings are concatenated into a single sequence of shape  $(1, N_{\text{total}}, D)$ , and a causal attention mask is applied to ensure that each segment only attends to other segments from the same time step. This enables efficient and correct attention computation without the overhead of padding. SegDAC is only limited by available memory for the maximum number of segments it can process.